Award Number: W81XWH-12-1-0093

TITLE: Novel Approaches to Breast Cancer Prevention and Inhibition of Metastases

PRINCIPAL INVESTIGATOR: Prof. Dr. Josef Penninger

CONTRACTING ORGANIZATION: IMBA – Institut fuer Molekulare Biotechnologie GmbH Vienna 1030

REPORT DATE: October 2016

TYPE OF REPORT: Annual Report

PREPARED FOR: U.S. Army Medical Research and Materiel Command
Fort Detrick, Maryland 21702-5012

DISTRIBUTION STATEMENT: Approved for Public Release;
Distribution Unlimited

REPORT DOCUMENTATION PAGE

Form Approved
OMB No. 0704-0188

1. REPORT DATE	2. REPORT TYPE	3. DATES COVERED
October 2016	Annual	30 Sep 2015 - 29 Sep 2016

4. TITLE AND SUBTITLE

Novel Approaches to Breast Cancer Prevention and Inhibition of Metastases

5a. CONTRACT NUMBER

5b. GRANT NUMBER
W81XWH-12-1-0093

5c. PROGRAM ELEMENT NUMBER

6. AUTHOR(S)

Prof. Dr. Josef Penninger

E-Mail: Josef.Penninger@imba.oeaw.ac.at

5d. PROJECT NUMBER

5e. TASK NUMBER

5f. WORK UNIT NUMBER

7. PERFORMING ORGANIZATION NAME(S) AND ADDRESS(ES)

IMBA – Institut fuer Molekulare Biotechnologie GmbH
Dr. Bohrgasse 3
Wien 1030
Austria

8. PERFORMING ORGANIZATION REPORT

9. SPONSORING / MONITORING AGENCY NAME(S) AND ADDRESS(ES)
U.S. Army Medical Research and Materiel Command
Fort Detrick, Maryland 21702-5012

10. SPONSOR/MONITOR'S ACRONYM(S)

11. SPONSOR/MONITOR'S REPORT NUMBER(S)

12. DISTRIBUTION / AVAILABILITY STATEMENT
Approved for Public Release; Distribution Unlimited

13. SUPPLEMENTARY NOTES

14. ABSTRACT

Technologies such as transcriptional profiling, genome sequencing, epigenetic, proteomic or metabolomic profiling have resulted in large sets of genome wide data. However, most of these datasets are of correlative. Functional and phenotypic annotation of the genome is thus a key challenge for a fundamental understanding of physiology and disease pathogenesis. We combine genetic model organisms and repairable mutagenesis with *in vivo* mouse genetics and human cohort studies to functionally characterize candidate breast cancer genes. Using mouse genetics, we showed that RANKL and its receptor RANK are critical regulators of sex hormone and BRCA1 mutation-driven breast cancer, providing a rationale for cancer prevention trials. We now provide human serology data that the RANKL/RANK system is deregulated in post-menopausal women at high risk for breast cancer and in women with circulating tumor cells. Thus, serum levels of RANKL are potentially indicative of predisposition and progression of breast cancer in humans. We also identified the small peptide Apelin as a key regulator of tumor neo-angiogenesis that cooperates with VEGFR in blood vessel growth in vitro engineered vasculature and in vivo in breast cancer. Inactivation of Apelin in a mammary cancer model reduces tumor blood vessels, reduced vascular leakage due to VEGFR-blocking therapy, and reduced metastases, thereby enhancing overall survival.

15. SUBJECT TERMS

Genome wide functional genetics, RANKL/RANK, breast cancer prevention, cancer angiogenesis, Apelin, VEGFR, metastases

16. SECURITY CLASSIFICATION OF:			**17. LIMITATION OF ABSTRACT**	**18. NUMBER OF PAGES**	**19a. NAME OF RESPONSIBLE PERSON** USAMRMC
a. REPORT U	**b. ABSTRACT** U	**c. THIS PAGE** U	UU	39	**19b. TELEPHONE NUMBER** *(include area code)*

Table of Contents

Page

INTRODUCTION

To capitalize on the breakthroughs in human genetics, I propose to take the next step into the post-genome era of cancer, i.e. to develop systems to rapidly assess the function of candidate genes in breast cancer pathogenesis and metastases. We will utilize the power of fly genetics combined with our unique Drosophila libraries to rapidly validate the function of hundreds and even thousands of human candidate breast cancer genes in epithelial transformation and metastases. Once these genes have been validated in fly, we will address their function in mammary cancer and metastases in mice using an entirely novel tool: my laboratory developed haploid embryonic stem cells. This technology allows us now to generate a library of murine ES cell clones that carry homozygous mutations in essentially all protein coding genes. Combining this mutant haploid ES cell library with in vivo mammary cancer and metastases assays, we will be able to rapidly **assess the role of novel candidate breast cancer genes**. In addition to finding essential new cancer pathways using fly and murine haploid ES cell technologies, I propose a project that could fulfill the dream of eradication of breast cancer and could have immediate impact on prevention and treatment of breast cancer, i.e. **to further explore the role of RANKL/RANK in breast cancer**. Moreover, I propose to take the RANKL/RANK system into human breast cancer patients to provide a novel prognostic marker for breast cancer risk and a molecular rationale for the initiation of clinical trials using already approved RANKL blockade as a tool to prevent the onset of breast cancer.

BODY

1. Explore the role of RANKL/RANK in breast cancer.

Background. RANKL (receptor activator of NF-kB ligand), its receptor RANK, and the decoy receptor osteoprotegerin (OPG) are essential for the development and activation of osteoclasts [1, 2]. Based on these findings, RANKL inhibition with a fully human, blocking monoclonal antibody (Denosumab) has been developed as a novel and rational therapy against osteoporosis

and skeletal related events in cancer patients [3-7]. RANKL/RANK also control lymph node organogenesis and the development of thymic medullary epithelial cells [1, 8, 9]. In addition, we have previously shown that the RANKL/RANK system is essential for the formation of a lactating mammary gland during pregnancy [10, 11] indicating that RANKL/RANK play a role in normal mammary gland biology and hormone-driven epithelial proliferation. Indeed, using genetic mouse-models, our group and Gonzalez-Suarez *et al*. have identified the RANKL/RANK system as a key regulator of hormone (progestin) and oncogene (Neu)-driven breast cancer [12, 13]. Moreover, we [14] and others [15] have recently reported that RANKL/RANK also control breast cancer development in scenarios of BRCA1 mutations. Mechanistically, RANKL/RANK promote the proliferation of human and mouse mammary gland epithelial cells, protect these cells from apoptotic cell death after DNA damage, control tumor stem cell renewal, and might have a role in basic mammary stem cell biology [12-18]. Furthermore, RANKL/RANK have also been implicated in metastases [12, 13, 19, 20].

Breast cancer is the most common female cancer, affecting approximately one in eight women during their life-time in North America and Europe [21, 22]. Identifying a biomarker which serves as both an indicator for breast cancer risk and at the same time a possible target for prevention is one of the most important yet unsolved needs. RANKL is expressed in primary breast cancers in patients and human breast cancer cells lines (14-19, 23] and, in mouse studies, the RANKL/RANK system is an important molecular link between progestins and oncogene-driven epithelial carcinogenesis [12, 13]. We therefore hypothesized that serum levels of RANKL and OPG could serve as markers for breast cancer risk providing a molecular rationale for future breast cancer prevention.

Results. In order to test whether deregulation of the RANKL/OPG system is associated with breast cancer in women without known genetic predispositions, we analyzed serum levels in postmenopausal women participating in the prospective UKCTOCS (UK Collaborative Trial of Ovarian Cancer Screening) study [24, 25]. This cohort of women provided a unique opportunity to study changes in serum levels of soluble RANKL and OPG well in advance of breast cancer

manifestation. A total of 278 samples from postmenopausal women were analyzed: 40 women donated a serum sample between 5 and 12 months prior to breast cancer diagnosis (median age at sample taken 64.84), 58 women provided sera between 12 and 24 months prior to breast cancer diagnosis (median age at sample taken 60.49 years) and 180 women, who did not develop breast cancer during their follow up (median age at sample taken 62.94 years), served as controls.

We did not observe significant differences in RANKL, OPG or RANKL-to-OPG ratios in controls and women who developed breast cancer 12–24 months after serum sampling. Since we have previously shown that RANKL mediates progesterone driven mammary epithelial proliferation [12] and the RANKL/RANK system is a key mediator of progestin-driven breast cancer in mouse models [12, 13], we explored a potential connection between progesterone and RANKL/OPG levels in humans. Intriguingly, we observed an increase of RANKL serum levels with increasing progesterone levels in women who developed breast cancer 12-24 months after sample collection (Figure 1A) and the opposite trend in controls. In the same cohort, we also observed a non-significant negative correlation of progesterone with OPG serum levels (Figure 1B) resulting in a significant alteration in the RANKL/OPG ratio among women with high serum progesterone (Figure 1C).

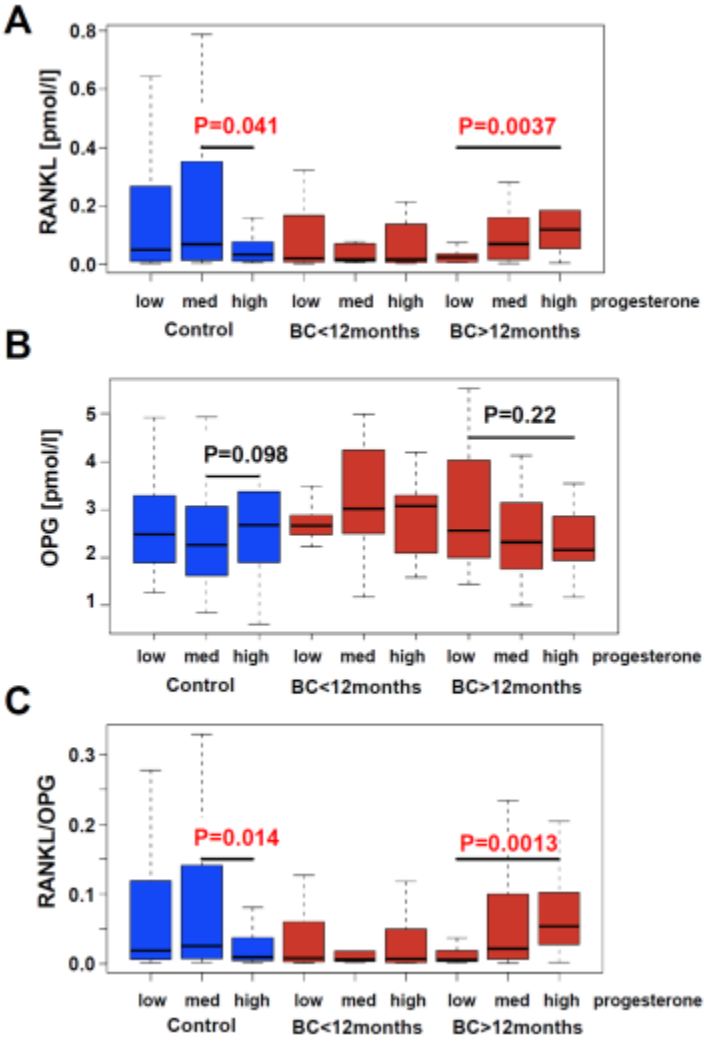

Figure 1. RANKL/OPG serum levels in human breast cancer patients. Analysis of RANKL (A), OPG (B) and the ratio RANKL/OPG (C) in relation to progesterone levels in prospectively collected UKCTOCS serum samples from 180 healthy postmenopausal women who did not develop breast cancer during their follow up and 40 healthy age-matched women who developed estrogen receptor positive breast cancer 5-12 months after their serum was collected as well as 58 healthy age-matched women who did develop ER-positive breast cancer 12-24 months after their serum was collected. Women were grouped according to their serum progesterone levels. Subjects were stratified into breast cancer patients and controls due to self reporting and histological examination. We have tested differences in RANKL, OPG and RANKL/OPG within each group between low versus medium and medium versus high progesterone within each group using the Mann Whitney U test and displayed only the significant p-values ($p<0.05$).

To assess whether high progesterone and high RANKL indeed define a subgroup of women with increased risk of developing breast cancer, we classified all women - cases and controls considered together - into tertiles according to their serum progesterone levels. Within each

group women were classified into low, medium or high RANKL, OPG and RANKL/OPG based on controls within the corresponding progesterone group. Using logistic regression women with high progesterone and high RANKL exhibited a 4.8 (95% CI 1.3 – 22.8; p=0.0269) fold risk (Table 1).

Table 1. Association of serum progesterone and RANKL with risk of breast cancer.

Progesterone LOW (range 0.03 - 0.19 ng/ml)																
RANKL [pmol/l]			Controls		Breast Cancer < 12 months						Breast Cancer > 12 months					
Tertile	Range		N (%)		N (%)		OR (95% CI)			p-value	N (%)		OR (95% CI)			p-value
1st	0.003	0.0193	21	33.9	7	50.0	1(ref)				6	42.9	1(ref)			
2nd	0.0193	0.179	20	32.3	4	28.6	0.60	0.1	2.3	0.47	8	57.1	1.40	0.4	4.9	0.59
3rd	0.179	3.716	21	33.9	3	21.4	0.43	0.1	1.8	0.26	0	0.0	0.00	NA		0.99

Progesterone MEDIUM (range 0.19 - 0.31 ng/ml)																
RANKL [pmol/l]			Controls		Breast Cancer < 12 months						Breast Cancer > 12 months					
Tertile	Range		N (%)		N (%)		OR (95% CI)			p-value	N (%)		OR (95% CI)			p-value
1st	0.004	0.0255	18	32.1	6	60.0	1(ref)				8	34.8	1(ref)			
2nd	0.0255	0.1745	19	33.9	3	30.0	0.47	0.1	2.1	0.34	9	39.1	1.07	0.3	3.4	0.91
3rd	0.1745	1.5235	19	33.9	1	10.0	0.16	0.0	1.0	0.10	6	26.1	0.71	0.2	2.4	0.59

Progesterone HIGH (0.31 - 12.68 ng/ml)																
RANKL [pmol/l]			Controls		Breast Cancer < 12 months						Breast Cancer > 12 months					
Tertile	Range		N (%)		N (%)		OR (95% CI)			p-value	N (%)		OR (95% CI)			p-value
1st	0.0045	0.0135	20	32.3	5	31.3	1(ref)				3	14.3	1(ref)			
2nd	0.0135	0.0675	21	33.9	5	31.3	0.95	0.2	3.9	0.94	3	14.3	0.95	0.2	5.7	0.96
3rd	0.0675	1.2315	21	33.9	6	37.5	1.14	0.3	4.5	0.84	15	71.4	**4.76**	**1.3**	**22.8**	**0.03**

All women - cases and controls considered together – were classified into tertiles according to their serum progesterone levels. Within each group, women were classified into low, medium or high RANKL based on controls within the corresponding progesterone group. Using logistic regression odd ratios (ORs) and 95 % Confidence Intervals (CI) have been calculated using the lowest RANKL group as a reference. Cases have been considered separately according to the time to diagnosis (more than one year or less).

Importantly, women within the high progesterone and high serum RANKL/OPG ratio group carried a 5.3 (95% CI 1.5 – 25.4, p=0.0169) fold risk to develop breast cancer 12-24 months after diagnosis (Table 2). We also grouped the women into RANKL/OPG tertiles across all controls (not only within a given progesterone tertile) and again women within the high progesterone/high RANKL/OPG group had a 4.2 (95% CI 1.3 – 16.0, p=0.02) fold risk for developing breast cancer. Thus, high serum levels of RANKL and high serum progesterone stratify a

subpopulation of postmenopausal women without known genetic predisposition at high risk of developing breast cancer 12-24 months before diagnosis.

Table 2. Association of serum progesterone and RANKL/OPG ratio with risk of breast cancer.

Progesterone LOW (range 0.03 - 0.19 ng/ml)*

RANKL/OPG ratio			Controls		Breast Cancer < 12 months						Breast Cancer > 12 months					
Tertile$	Range		N (%)		N (%)		OR (95% CI)¶			P-value	N (%)		OR (95% CI)¶			P-value
1st	0.0014	0.0075	21	33.9	7	50.0	1(ref)				9	64.3	1(ref)			
2nd	0.0075	0.0644	20	32.3	4	28.6	0.60	0.1	2.3	0.47	5	35.7	0.58	0.2	2.0	0.40
3rd	0.0644	2.0472	21	33.9	3	21.4	0.43	0.1	1.8	0.26	0	0.0	0.00	NA	NA	1.0

Progesterone MEDIUM (range 0.19 - 0.31 ng/ml)*

RANKL/OPG ratio			Controls		Breast Cancer < 12 months						Breast Cancer > 12 months					
Tertile$	Range		N (%)		N (%)		OR (95% CI)¶			P-value	N (%)		OR (95% CI)¶			P-value
1st	0.0017	0.0154	19	33.9	6	60.0	1(ref)				8	34.8	1(ref)			
2nd	0.0154	0.091	18	32.1	4	40.0	0.70	0.2	2.9	0.63	9	39.1	1.19	0.4	3.8	0.77
3rd	0.091	0.4605	19	33.9	0	0.0	0.00	NA		0.99	6	26.1	0.75	0.2	2.6	0.65

Progesterone HIGH (0.31 - 12.68 ng/ml)*

RANKL/OPG ratio			Controls		Breast Cancer < 12 months						Breast Cancer > 12 months					
Tertile$	Range		N (%)		N (%)		OR (95% CI)¶			P-value	N (%)		OR (95% CI)¶			P-value
1st	0.0015	0.0057	21	33.9	6	37.5	1(ref)				3	14.3	1(ref)			
2nd	0.0057	0.0245	20	32.3	4	25.0	0.70	0.2	2.8	0.62	2	9.5	0.70	0.1	4.7	0.71
3rd	0.0245	0.4672	21	33.9	6	37.5	1.00	0.3	3.7	1.00	16	76.2	**5.33**	**1.5**	**25.4**	**0.02**

* All women - cases and controls considered together – were classified into tertiles according to their serum progesterone levels.

$ Within each progesterone tertile, women were classified into low, medium or high RANKL/OPG based on controls within the corresponding progesterone group.

¶ Using logistic regression odd ratios (ORs) and 95 % Confidence Intervals (CI) have been calculated using the lowest RANKL/OPG group as a reference. Cases have been considered separately according to the time to diagnosis (more than one year or less).

We next analyzed the group of UKCTOCS participants who developed breast cancer within 12 months (BC < 12 months). However, among this cohort high progesterone/high RANKL levels were not associated with an increased incidence of breast cancer (Figure 1, Table 2). Intriguingly, we rather observed a progesterone-independent reduction in RANKL and increase in OPG serum

levels with breast cancer manifestation resulting in significant decrease in the RANKL-to-OPG ratio compared to UKCTOCS participants who never developed breast cancer (Figure 2A). These results indicate that RANKL levels drop whereas OPG levels increase in women close to clinical manifestation of breast tumors. One possible explanation for this phenomenon could be that some women already harbor subclinical disseminated tumor cells that could lead to the observed alterations in serum RANKL/OPG.

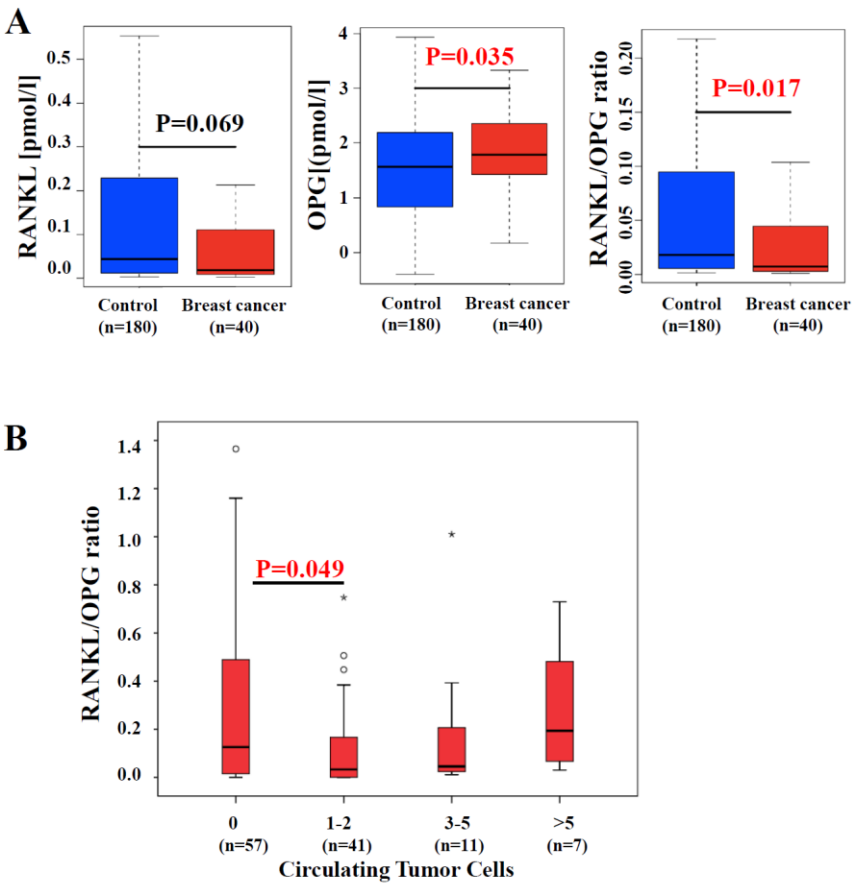

Figure 2. Alterations in RANKL/OPG levels in females close to onset and after manifestation of breast cancer. A. Analysis of OPG, RANKL, and RANKL/OPG ratios in prospectively collected UKCTOCS serum samples from 180 healthy postmenopausal women who did not develop breast cancer during their follow up (control) and 40 healthy age-matched women who developed ER positive breast cancer 5-12 months after their serum was collected. P values were calculated using a Mann Whitney U test. **B**. Analysis of RANKL/OPG ratios in 116 women in the SUCCESS trial *after resection* of the local ER positive breast cancer and *before start of systemic treatment* based on the numbers of CTCs. P values were calculated using the Mann Whitney U test. Abbreviations: CTC, circulating tumor cell; ER, estrogen receptor; OPG, osteoprotegerin; RANKL, Receptor Activator of NF-kB ligand.

To test this hypothesis, we analysed serum RANKL/OPG in women with breast cancer diagnosis but in the absence of a tumor in the breast – a similar scenario as in the UKCTOCS cohort close to breast cancer diagnosis. We analyzed 116 ER positive breast cancer patients from the SUCCESS trial after surgery and before systemic therapy. Figure 2B demonstrates serum RANKL/OPG levels stratified to the number of circulating tumor cells (CTCs) identified in the corresponding blood sample [26, 27]. Intriguingly, women with a small number of CTCs (1-2 CTCs) exhibited a significantly reduced serum RANKL/OPG ratio compared to women without detectable CTCs (Figure 2B). Women with a 3-5 CTCs also exhibited reduced serum RANKL/OPG ratios, though this reduction did not reach statistical significance. Of note, the serum RANKL/OPG ratio tends to increase again with an increase in CTCs, albeit the numbers of cases are too small to allow for a firm conclusion. Thus, women with a very low number of CTCs in their blood exhibit a reduced RANKL/OPG ratio suggesting that the alterations we find up to one year in advance of a clinical breast cancer indeed correlate with low numbers of disseminated breast cancer cells.

To substantiate these data in another entirely independent cohort, we determined RANKL and OPG serum levels of participants from the Bruneck study [28, 29], that allowed us to analyse matched patient samples before and after cancer manifestation. Of 821 subjects with two or more sequential measurements of RANKL and OPG, 697 subjects remained free of cancer during the 15-year follow-up, 19 women developed breast cancer, 16 men developed prostate cancer, and 89 other cancer types (all malignancies except for squamous-cell skin cancer). In line with the UKCTOCS study, levels of RANKL declined with the manifestation of breast cancer ($P=0.006$; paired t-test), whereas RANKL serum concentrations were not altered in subjects with other types of new-onset cancer and those remaining free of neoplastic disease (Figure 3A). In parallel, OPG levels rose with the diagnosis of breast cancer ($P=0.037$; paired t-test), whereas no such increase was observed in patients with other types of cancer or subjects free of neoplastic disease (Figure 3A). As a consequence, the RANKL-to-OPG ratio significantly decreased in individuals with new-onset breast cancer (Figure 3B). In males, no significant differences in OPG and RANKL levels were found in cancer-free individuals or those with new onset prostate cancer, which is also related to sex hormones, or other types of cancer. Our data in two different human prospective

breast cancer cohorts indicate that alterations in RANKL/OPG ratios are significantly associated with breast cancer manifestation.

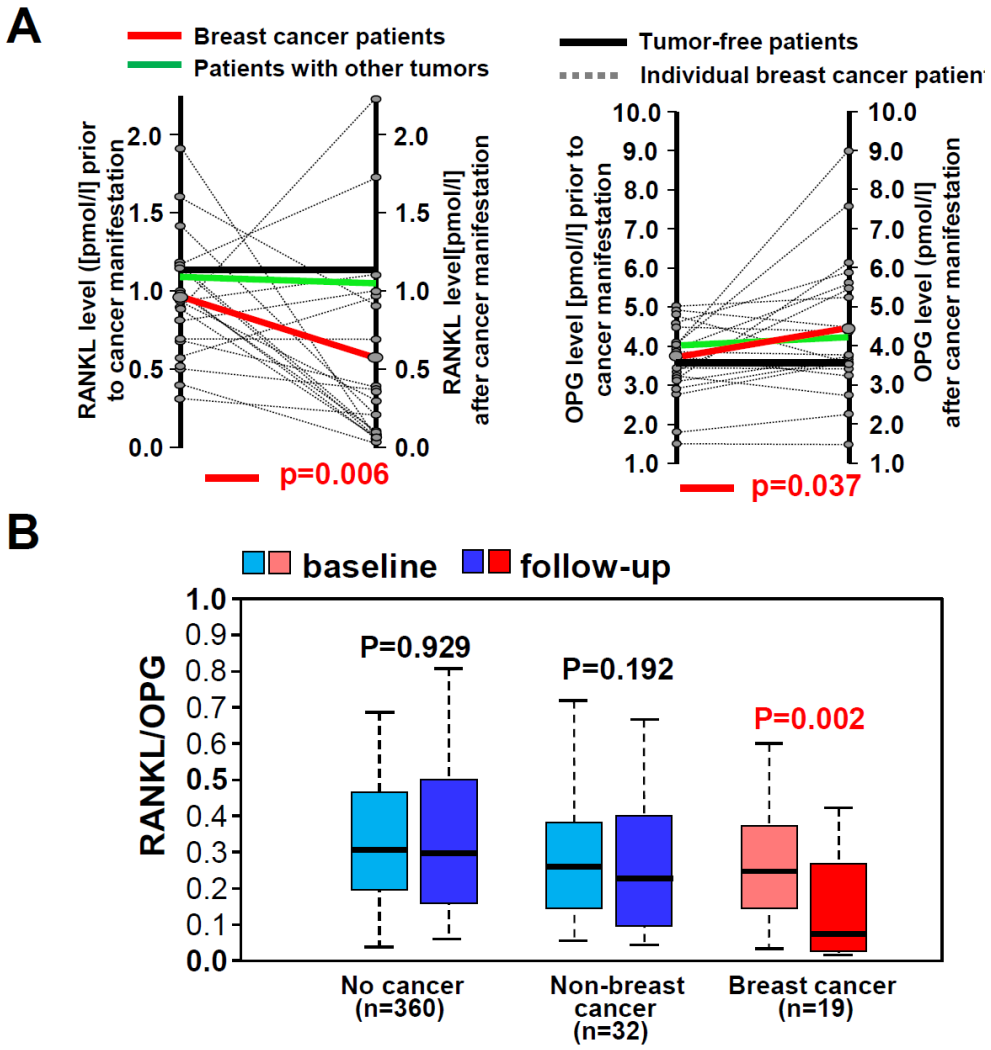

Figure 3. Alterations in RANKL/RANKL levels in females close to onset and after breast cancer. A. Individual changes in serum levels of OPG and soluble RANKL in 19 female subjects from our longitudinal Bruneck cohort before and after manifestations of breast cancer (dotted black lines). Mean changes are shown for subjects with incident breast cancer (red lines), other types of new-onset cancer (n=32; green lines) and women free of neoplastic disease during the 15 year follow-up (n=360; black lines). **B.** Box plots of RANKL-to-OPG ratios assessed prior to (hatched) and after (filled boxes) cancer manifestation in women from the prospective Bruneck study indicate median ratio levels and inter-quartile ranges. In individuals who remained free of cancer, ratios given are those assessed at the time intervals corresponding to those in cancer patients.

Discussion. We and other groups have previously demonstrated a central role for the osteoclastogenic molecule RANKL in breast cancer development using genetic mouse models [12-15]. Here we show that increased progesterone and RANKL serum levels stratify a subgroup of postmenopausal women without known genetic predispositions that exhibit a ~5 fold increased risk of developing breast cancer 12-24 months before cancer diagnosis. This indicates that either increased free RANKL or high RANKL and high progesterone serum levels, as seen in the case of our postmenopausal UK cohort, could be useful biomarkers to predict future breast cancer more than one year in advance of breast cancer diagnosis. These data are in line with our genetic mouse models that the RANKL/RANK/OPG system drives the initiation and progression of breast cancer [12-15]. Our findings that an increased RANKL/OPG ratio > 12 months prior to breast cancer development is consistent with data from meta-analysis showing that sex steroid hormone levels well in advance of breast cancer diagnosis are more significantly associated with breast cancer risk compared with hormone levels analyzed closer to diagnosis [30].

When we analyzed the serum of postmenopausal women shortly before breast cancer diagnosis or matched sera from women before and after clinical manifest breast cancer, we observed reduced RANKL and increased OPG serum levels. A similar phenomenon was shown for serum RANKL levels and osteoporosis: low serum RANKL levels are associated with a 10-fold higher risk of non-traumatic fractures in postmenopausal women [31]. Moreover, increased OPG is associated with enhanced bone loss in postmenopausal women not on hormone replacement therapy [32] and increased OPG levels have been observed in patients with bone metastasis [33]. The mechanisms of these serum changes in breast cancer need to be further investigated and might reflect compensatory mechanisms against developing microtumors and/or redistribution/sequestration of RANKL/OPG within different body compartments. Although women in our study do not have clinical manifest bone metastasis, it has been demonstrated that tumor cells can disseminate systemically from earliest epithelial alterations in transgenic mice and even from very early breast cancers in women and that these disseminated tumor cells can form micro-metastases in bone marrow and lungs [34]. Likewise, it is well established that breast cancer cells interfere with osteoblasts (being a major source for RANKL) and induce osteoblast necrosis and apoptosis [35]. Hence the effect we see on RANKL and the RANKL/OPG ratio in

women who get clinical manifest breast cancer close to serum collection may be triggered by an effect of epithelial/tumour cells altering RANKL/OPG in the bone marrow. Of note, recently it has been reported that blocking of RANKL reduces the reoccurrence of breast cancer in women receiving adjuvant Tamoxifen therapy [36].

One key issue for the management of cancer is to accurately predict the risk in order to triage women into screening or preventive strategies. In breast cancer, population-based mammography screening is currently used to identify women with early breast cancer. Our data suggest that the apparent alterations in RANKL/OPG in postmenopausal women with high progesterone levels could be used as a future biomarker to identify a subgroup of women at high risk of breast cancer. Moreover, it has been recently shown that women with high genetic breast cancer risk due to *BRCA1* mutations appear to be exposed to increased RANKL [37]. Our data also indicate that serum RANKL/OPG ratios correlate with CTCs and that a low number of CTCs – even in the absence of a local breast cancer – is associated with a reduced serum RANKL/OPG ratio. The mechanism of this phenomenon is not yet clear, but it is attractive to speculate that unknown soluble serum factors which are associated with a low number of CTCs may suppress RANKL expression and/or alter processing of membrane bound RANKL into soluble RANKL. These studies now need to be confirmed in additional cohorts. Since an antibody to block RANKL (Denosumab) has already been approved for treatment of osteoporosis patients and treatment of skeletal related events in solid tumors [3, 7], our data in the presented prospective human cohorts further support the notion that the same antibody could potentially be used to prevent the development of breast cancer in high risk women.

2. To assess the role of novel candidate breast cancer genes

Background. The activation of angiogenesis, the sprouting of new blood vessels from the existing vasculature, is one of the hallmarks of cancer and facilitates rapid tumour growth and metastasis [38]. During cancer progression, an 'angiogenic switch' is frequently activated, causing aberrant capillary sprouting, tortuous and excessive vessel branching, enlarged vessels, erratic blood flow, micro-haemorrhaging, leakiness, and abnormal levels of endothelial cell proliferation and apoptosis. Inhibition of this angiogenic switch is therefore a cancer treatment strategy. Given the importance of vascular endothelial growth factors (VEGFs) in angiogenesis, much attention has been focused on developing anti-VEGF signalling therapies to treat a variety of cancers by blocking tumour angiogenesis. Whereas various clinical trials have demonstrated the efficiency of these therapies [39], the benefits are usually transitory. The large scale eradication of tumour vessels results in necrosis and hypoxia, which triggers several resistance mechanisms that drive tumour regrowth and malignancy [39-41].

In recent decades, the concept of vessel normalization has been considered promising; this can be triggered by anti-angiogenic therapy and leads to the repair of vascular abnormalities with vessels becoming less permeable and better perfused [42]. Promoting vessel normalization has been linked to decreased metastasis and an increased efficacy of chemotherapies and immune therapies [43]. However, VEGF inhibitors lead to a transient, usually rather short period of vessel normalization as they cannot be finely tuned to achieve permanent normalization without reducing the tumour vasculature to such an extent that hypoxia recurs and, at this point, acquired resistance emerges [44]. There is a need for new agents that can potentiate VEGF pathway blockers' ability to reduce primary tumour growth and complement it with a reduction in tumour regrowth and malignancy.

Results. Current anti-angiogenic therapies are based only on the inhibition of tyrosine kinase receptors (RTK), of which VEGFR2 is the common denominator. In contrast, apelin is an evolutionarily conserved peptide that acts as the endogenous ligand for the G-protein-coupled apelin receptor [45]. The apelin/apelin receptor signalling pathway plays a relevant role in

developmental angiogenesis and vascular development [46-53]. While the pathway is downregulated in adulthood, it is frequently found to be upregulated in tumours [54,55] and tumour endothelial cells [56]. As targeting the apelin signalling pathway is a different approach to targeting RTKs, we investigated whether specific blockage of the apelin/apelin receptor pathway could be an alternative to current RTK inhibitor (RTKI) anti-angiogenic therapy, or an accompaniment to this therapy that could offer lower resistance and lower overall toxicity.

Unbiased meta-analysis of multiple datasets using the Kmplot and PrognoScan databases showed that high levels of apelin expression are significantly associated with poor prognosis in breast cancer (Figure 4A,B). To study the potential for improving prognosis through blockage of apelin expression in mammary cancer, we intercrossed apelin-deficient (*Apln*$^{-/-}$) mice [57] with MMTV-*NeuT* transgenic mice [58] to generate MMTV-*NeuT;Apln*$^{-/-}$ and MMTV-*NeuT;Apln*$^{+/+}$ mice (termed *NeuT;Apln*$^{-/-}$ and *NeuT;Apln*$^{+/+}$ hereafter). The *Apln*$^{-/-}$ mouse is a whole body knockout and therefore mimics the effect of targeting apelin in the whole body. Apelin-null mice showed a significant prolonged survival compared with their wild type counterparts after tumour onset (Figure 4C), showing that the apelin signalling pathway is a promising target for cancer treatment. Accordingly, age-matched apelin-null littermates presented a decreased percentage of tumour burden in the mammary glands (Figure 4D). Similar results were found in a mouse model of metastatic mammary cancer (E0771 cells) where apelin was interfered and cells were orthotopically injected into the mammary glands of C57B6/J *Apln*$^{-/-}$ mice (Figure 4E). To extend these results, we then analysed age-matched NeuT-positive tumours and found that tumours without apelin had a significantly decreased microvessel density (Figure 4F). Together, these data show that blocking apelin signalling is an effective strategy to reduce tumour angiogenesis and increase survival in mice with mammary and lung cancer, both cancers in which high apelin levels are correlated with a worse prognosis in humans.

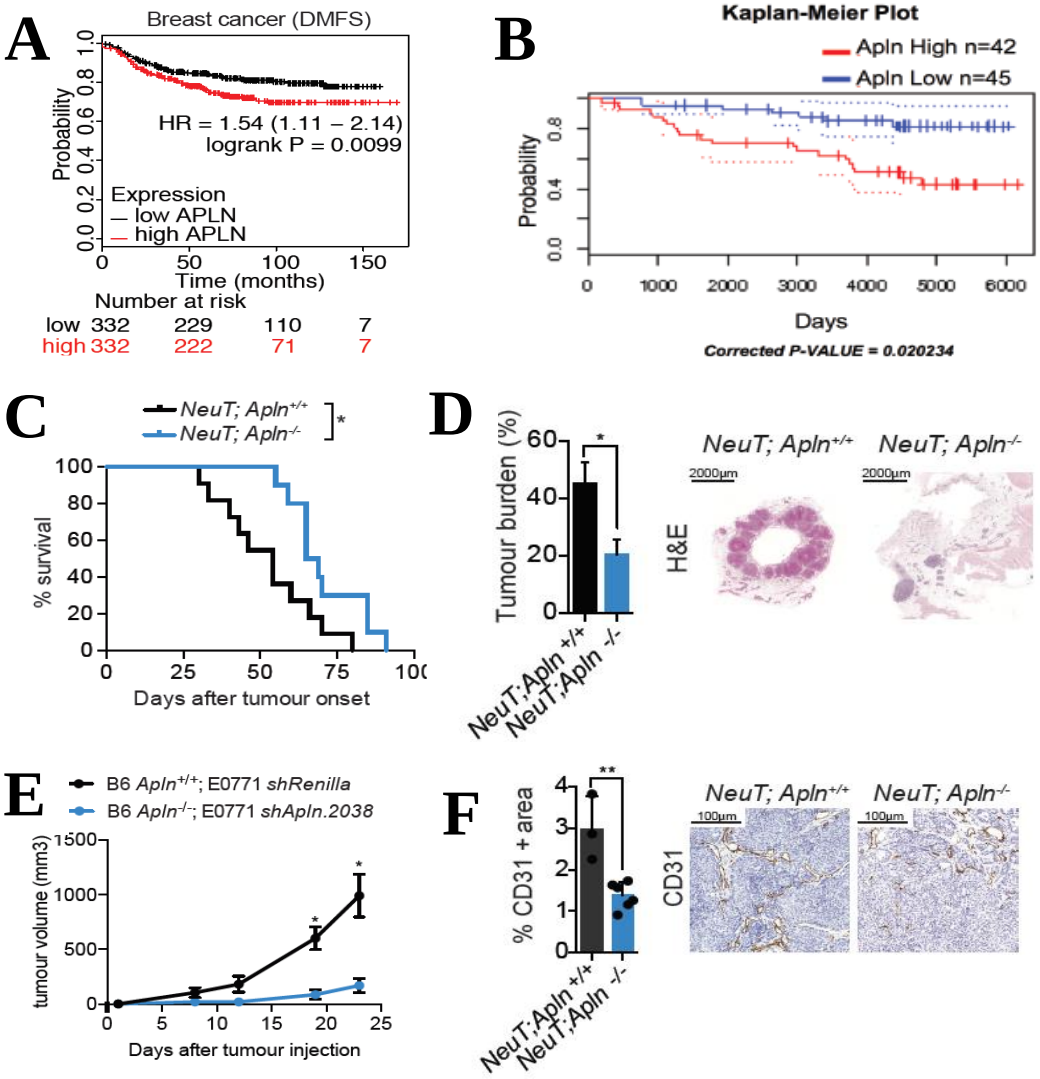

Figure 4. Apelin targeting improves survival and reduces angiogenesis in breast cancer. A, Kaplan Meier plot for high and low apelin-expressing human breast cancer patients. Patients were split by the median. Affymetrix probe ID 222856_at. DMFS=distant metastasis free survival. **B**, Kaplan Meier plots for high and low apelin-expressing groups in human breast cancer from Prognoscan filtered by significant corrected P-value and Cox P-value. Dataset GSE6532-GPL570, distant metastasis free survival. **C,** Kaplan Meier plot for survival in *NeuT;Apln*$^{+/+}$ (n=11) and *NeuT;Apln*$^{-/-}$ (n=10) mice with mammary cancer after tumor onset (*P<0.05; Log rank test). Mice were sacrificed when the tumour size was 1-1.5cm^3, following the ethical guidelines. **D**, Percentage of tumor burden in 4 weeks age-matched *NeuT;Apln*$^{+/+}$ (n=6) and *NeuT;Apln*$^{-/-}$ (n=9) mammary glands (*P<0.05; t test). Data are shown as means ± s.e.m. Representative H&E images are shown. **f**, Tumor burden in 14 weeks age-matched *KRas;Apln*$^{+/y}$ (n=4) and *KRas;Apln*$^{-/y}$ (n=7) lungs (*P<0.05; t test). Data are means ± s.d. Representative H&E images are shown. **E,** Tumor volume followed over-time from E0771 cells control (*shRenilla*) or apelin-interfered (*shApln.2038*) orthotopically-injected in C57B6/J *Apln*$^{+/+}$ or *Apln*$^{-/-}$ mice. Data are means ± s.e.m (n=3; *P<0.05, multiple t tests). **F,** CD31-positive area in *NeuT;Apln*$^{+/+}$ (n=3) and *NeuT;Apln*$^{-/-}$ (n=6) 4 weeks age-matched mammary tumours. Data are means ± s.d. (**P<0.005; t test). Representative images are shown.

Apelin is an angiogenic factor specifically upregulated in both tumour and tumour endothelial cells [56,59,60]. As in human cancer [54], we found that apelin expression is enhanced in mouse NeuT-positive tumoral tissue compared with the mammary gland of healthy mice (Fig. 5A). We found that the apelin receptor is similarly expressed in normal epithelial mammary cells and *NeuT;Apln*$^{+/+}$ mammary tumours, and it is less expressed in *NeuT;Apln*$^{-/-}$ tumour samples (Fig. 5B), probably owing to the absence of the ligand. Additionally, we were able to detect an increase in *Apln* and *Aplnr* expression in tumour endothelial cells compared with normal endothelial cells (Fig. 5C,D). Although we explored whether *Apela*, the recently described ligand for apelin receptor [61], was also overexpressed in NeuT and E0771 mammary tumours, we could barely detect expression, thus establishing apelin as the main upregulated apelin receptor ligand in our models of mammary and lung cancer. We could not detect any abnormality in mammary glands from non-tumour-bearing adult *Apln*$^{+/+}$ and *Apln*$^{-/-}$ mice (Fig. 5E)

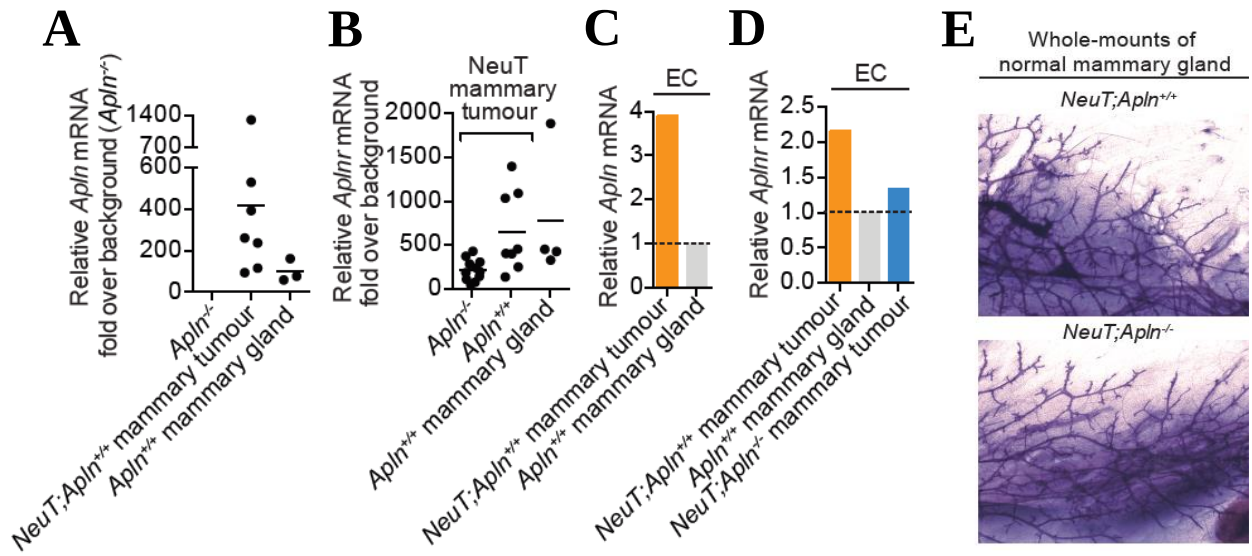

Figure 5. Apelin expression in mammary tumor cells. A and **B**, RT-qPCR of apelin and apelin receptor from *NeuT;Apln*$^{+/+}$ tumors and normal mammary glands and NeuT;Apln$^{-/-}$ tumors. **C** and **D**, RT-qPCR of apelin and apelin receptor from endothelial cells (ECs) isolated from *NeuT;Apln*$^{+/+}$ tumours and normal mammary glands and *NeuT;Apln*$^{-/-}$ tumours. **E**, Representative whole-mount images from *Apln*$^{+/+}$ or *Apln*$^{-/-}$ mammary glands.

To elucidate the mechanism by which apelin ablation reduces tumour burden and angiogenesis, we used the E0771 orthotopic mammary cancer model to specifically downregulate *Apln* and *Aplnr* in cancer cells only. When injected in C57B/6J wild type mice (B6 hereafter), only *Apln*-interfered (*shApln*) E0771 cells (Figure 6A) showed significantly reduced cell growth (Figure 6B,C) and vessel density (Figure 6D) compared with control *shRenilla*-expressing (*shRen*) E0771 cells. Apelin receptor interference (*shAplnr*) did not show any reduction in tumour growth or vessel density compared with *shRen*-expressing control cells (Figure 6A-D), pointing towards an exclusive paracrine action of apelin to stimulate vessel recruitment and tumour growth. Accordingly, the morphology and proliferation of E0771 cells, control or interfered for apelin or apelin receptor, *in vitro* was unaffected (Figure 6E,F), even when the cells were stimulated with an active form of apelin (AplnPyer13) or when they were under hypoxic conditions.

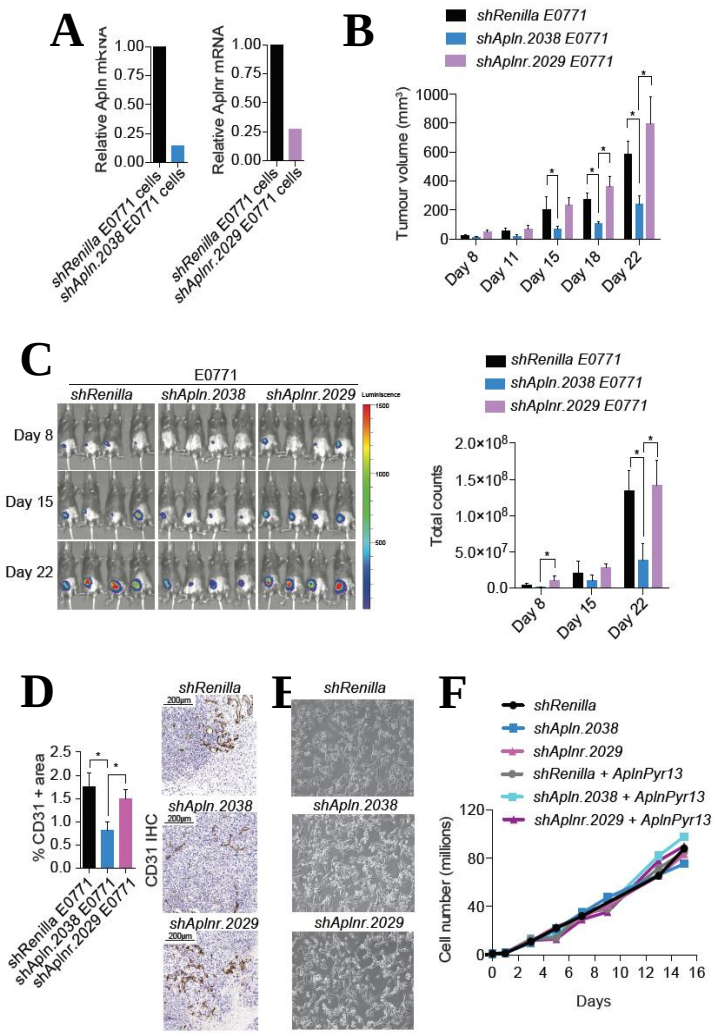

Figure 6. Apelin control mammary tumor growth in the E0771 orthotopic breast cancer model. A, RT-qPCR of apelin and apelin receptor in E0771 control cells (*shRenilla*) and apelin or apelin receptor-interfered cells (*shApln.2038* and *shAplnr.2029*, respectively). **B**, Tumour volume followed over-time from E0771 cells control (*shRenilla*), apelin-interfered (*shApln.2038*) and apelin receptor-interfered (*shAplnr.2029*) orthotopically-injected in C57B6/J mice. Data are mean ± s.e.m (n=3-4; *P<0.05, multiple t tests). **C**, Bioluminiscence image and quantification of mammary tumors from orthotopically-injected E0771 cells *shRenilla*, *shApln.2038* or *shAplnr.2029* in C57B6/J mice at day 8, 15 and 22 post-injection. Data are means ± s.e.m (n=4, *P<0.05, multiple t tests). **D**, CD31+ area of E0771 tumours at day 12 post injection. Representative staining images are shown. Data are shown as means ± s.e.m (n=6-7; *P<0.05; t test). **E**, Representative images of E0771 cells *shRenilla*, *shApln.2038* or *shAplnr.2029* in culture (20x). **F**, Growth curve of E0771 cells *shRenilla*, *shApln.2038* or *shAplnr.2029* in absence or presence of apelin peptide (AplnPyr13).

The orthotopic injection of apelin-interfered E0771 breast cancer cells into *Apln*$^{+/+}$ or *Apln*$^{-/-}$ mice showed a tendency towards major reduction of tumor growth in the latter compared with the former (Figure 7A), suggesting that the blockage of apelin production not only in tumour cells but also in the tumor microenvironment would be therapeutically beneficial, although tumour apelin seems to play the predominant role in tumour progression. Orthotopic injection of E0771 *shApln* cells into *Apln*$^{-/-}$ mice not only reduced vessel density but also vessel leakage (Figure 7B,C), which is a major undesirable effect of current RTKI anti-angiogenic therapy.

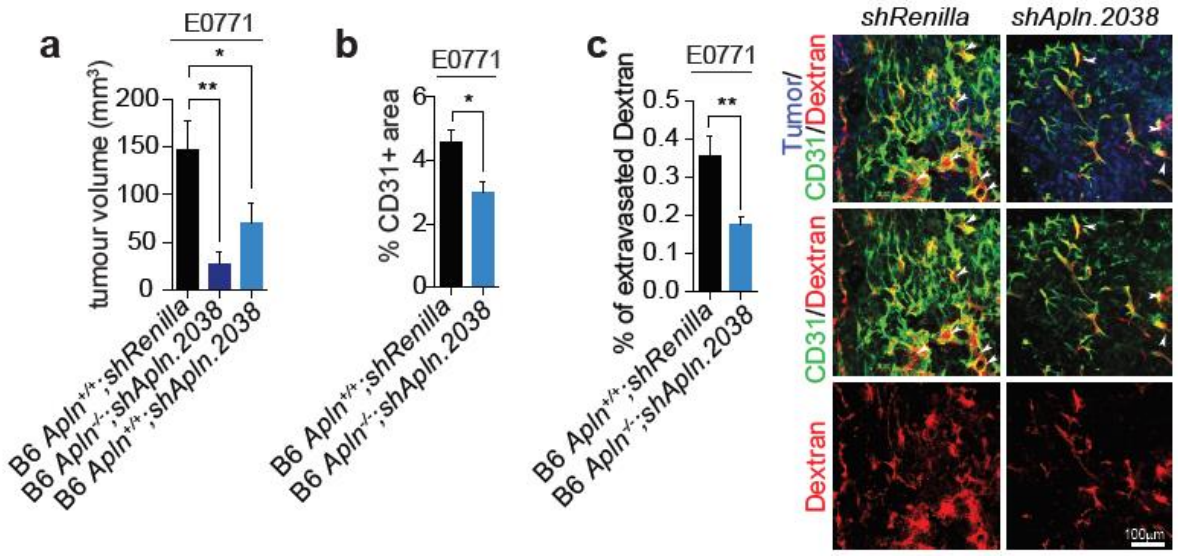

Figure 7. Apelin controls breast cancer growth and tumor vessel leakage. A, Tumor volume of *shRenilla* or *shApln.2038* E0771 tumours at day 12 post orthotopic injection in C57B6/J *Apln*$^{+/+}$ or *Apln*$^{-/-}$ mice. Data are means ± s.e.m (n=6-12; *P<0.05; **P<0.005; one-way ANOVA to *shRenilla*). **B**, Percentage of CD31+ area of age-matched mammary tumors (day 23) from E0771 cells control (*shRenilla*) or apelin-interfered (*shApln.2038*) orthotopically-injected in C57B6/J *Apln*$^{+/+}$ or *Apln*$^{-/-}$ mice. Data are means ± s.e.m (n=3; *P<0.05, t test). **C**, Percentage of extravasated Dextran in age-matched mammary tumours (day 19) from E0771 cells control (*shRenilla*) or apelin-interfered (*shApln.2038*) orthotopically-injected in C57B6/J *Apln*$^{+/+}$ or *Apln*$^{-/-}$ mice, respectively. Representative immunofluorescence stainings of Dextran (red) and CD31+ vessels (green) are shown. Data are means ± s.e.m (n=9-12; **P<0.005; t test).

Having observed that apelin blockage can reduce vessel angiogenesis, and given that apelin receptor is a G-protein coupled receptor (GPCR) and not an RTK, we studied whether apelin had an effect on VEGF-induced angiogenesis using an established *in vitro* system of 3D vessel sprouting from embryoid bodies (EBs) upon VEGF stimulation [62]. Although apelin stimulation

alone was not sufficient to initiate the vessel sprouting, we observed that apelin strongly boosted the vessel sprouting initiated by VEGF. We next generated *Apln*$^{-/-}$ mouse embryonic stem cells (mESCs) using a gene-trap strategy in haploid stem cells [63] that can be reversed to *Apln*$^{+/+}$ by Cre expression. Cre expression does not affect vessel sprouting. Whereas *Apln*$^{-/-}$ mESCs grew normally, *Apln*$^{-/-}$ EBs presented delayed sprouting upon VEGF treatment compared with wild type controls (Figure 8A). We also performed competition assays in which chimeric EBs 1:1 from *Apln*$^{+/+}$ (mCherry+-Cre): *Apln*$^{-/-}$ (GFP+) mESCs were stimulated with VEGF. Chimeric EBs showed a significant decrease in the total amount of *Apln*$^{-/-}$ endothelial cells compared with *Apln*$^{+/+}$ endothelial cells by FACS analysis (Figure 8B), thereby confirming the functional disadvantage of apelin-null cells in vessel sprouting. Confocal microscopy further showed that *Apln*$^{-/-}$ endothelial cells are significantly less prone to occupy a tip-cell position compared with wild type endothelial cells during VEGF-induced angiogenesis (Figure 8C). We also performed transcriptome analysis of CD31+ endothelial cells from sprouting EBs in the presence (*Apln*$^{+/+}$) or absence (*Apln*$^{-/-}$) of apelin upon VEGF stimulation. Ingenuity Pathway Analysis (IPA) showed that, in absence of apelin, the top inhibited disease and function category is angiogenesis (Figure 8D). Most VEGF-target genes inhibited in the absence of apelin are angiogenesis-related genes. These results show that apelin is required to fully activate VEGF-target genes in endothelial cells, which is important for proper angiogenesis.

We finally performed unbiased pathway analysis by phospho-kinase array in primary human endothelial cells to further characterize the signalling pathways regulated by apelin and VEGF. Unstimulated control cells and cells stimulated with an active apelin peptide, recombinant VEGF or both were subjected to analysis on 43 kinase phosphorylation sites simultaneously (Figure 8E). While VEGF stimulation activated pathways that are known to be involved in endothelial cell proliferation and vessel permeability (such as FAK, β-Catenin, PYK2, ERK1/2, Src, Fyn or Yes), apelin also proved its ability to activate these pathways in endothelial cells. In some situations, the addition of both ligands further activated specific pathways, showing a synergistic effect from both signalling pathways. These data show that both apelin and VEGF regulate

pathways in endothelial cells to stimulate angiogenesis and also vessel permeability, which has been linked to tumor malignancy, extravasation and metastasis [64].

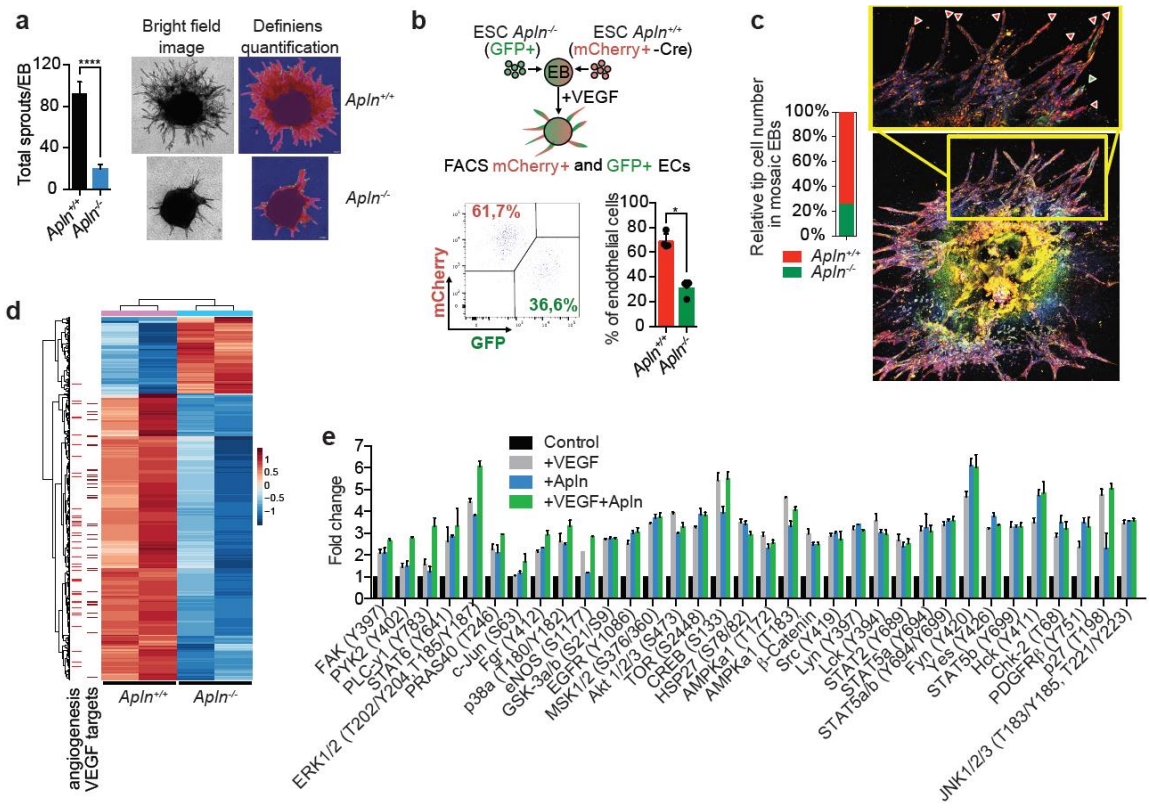

Figure 8 Apelin synergizes with VEGF to induce vessel sprouting. A, Number of vessel sprouts per embryoid body (EB) formed from *Apln*$^{+/+}$ or *Apln*$^{-/-}$ mouse embryonic stem cells (mESCs) 5 days after initiation of the vessel sprouting upon VEGF treatment. Data are shown as means ± s.e.m. (n=13-14; ****P<0.0005, Mann-Whitney test). Representative images are shown. Left image: Bright field picture of sprouting EBs. Right image: Vessel sprouts automatic quantification using Definiens software followed by manual correction. **B**, Percentage of CD31+ endothelial cells (ECs) evaluated by FACS from mosaic EBs formed of 1:1 ESCs *Apln*$^{+/+}$ (mCherry+-Cre): ESCs *Apln*$^{-/-}$ (GFP+) (*P<0.05, Mann-Whitney test; n=4). Data are shown as means ± s.d. Representative FACS analysis is shown. **C**, Relative number of tip cells occupied by an *Apln*$^{+/+}$ (mCherry+-Cre) or *Apln*$^{-/-}$ (GFP+) cell. 43 sprouts were counted. **D**, Differentially expressed genes in RNAseq analysis of CD31+ ECs isolated from sprouting EBs from either *Apln*$^{-/-}$ cells stimulated with VEGF (total absence of Apelin) or *Apln*$^{+/+}$ stimulated with VEGF and Apelin (full presence of Apelin). **E**, Phospho-kinase array in primary human umbilical venous endothelial cells (HUVECs) stimulated for 5' with VEGF, apelin (AplnPyr13) or both. The results are shown as fold-changed from the unstimulated control.

Despite the promise of anti-VEGF and multitargeted pan-VEGF RTKI anti-angiogenic therapy, resistance remains one of the key issues related to its failure [41]. To study whether apelin blockade could complement current RTKI anti-angiogenic therapies, we administered the

multitargeted pan-VEGF RTKI sunitinib (Sutent) to *NeuT;Apln*$^{-/-}$ and *NeuT;Apln*$^{+/+}$ mice upon mammary tumor onset. Sunitinib treatment has been widely studied in preclinical and clinical settings and is well-known as a potent inhibitor of tumour angiogenesis and tumour growth, especially in sustained treatment [65,66]. Apelin ablation combined with sunitinib treatment significantly increased survival from tumor onset (Figure 9A). Age-matched samples showed a significant reduction of tumoural tissue in the combinatory situation (Figure 9B). To normalize the data, we size-matched NeuT+ mammary tumors at an early stage (20–70mm^3) using MRI, which were untreated or treated with sunitinib until the day of sacrifice and followed over time. MRI analysis showed that sunitinib treatment decreases the rate of tumor growth. *NeuT;Apln*$^{-/-}$ tumors presented a similar growth rate. Sunitinib-treated *NeuT;Apln*$^{-/-}$ tumors showed a pronounced decrease in growth, which was confirmed by mitotic count and PHH3 immunostaining 6 weeks after tumors were size-matched – or 4 weeks after in the case of some *NeuT;Apln*$^{+/+}$ sacrificed early owing to the large size of their tumors, when all tumors except for the sunitinib-treated *NeuT;Apln*$^{-/-}$ tumours presented similar growth rates (Figure 9C,D).

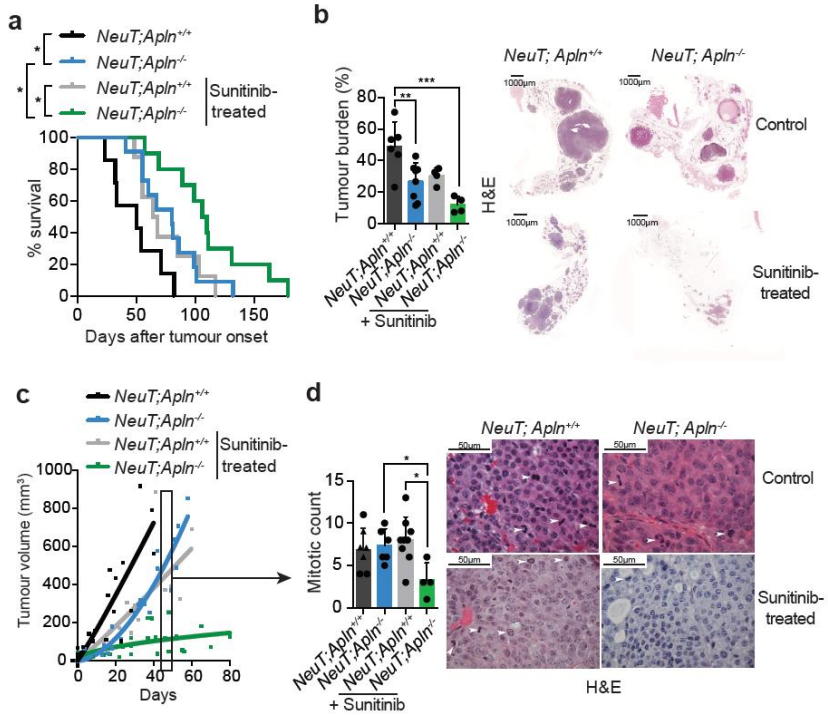

Figure 9. Combination of apelin and RTK blockage improves survival in breast cancer. A, Kaplan Meier plot for survival in *NeuT;Apln*$^{+/+}$ and *NeuT;Apln*$^{-/-}$ mice with mammary cancer, control or treated with sunitinib malate (60mg/kg per dose) three times a week after tumour onset (n=7-11; *P<0.05; Log rank test). Mice were sacrificed when the tumour size was 1-1.5cm^3, following the ethical guidelines. **B,** Percentage of proliferative area in 4 weeks age-matched *NeuT;Apln*$^{+/+}$ and *NeuT;Apln*$^{-/-}$ mammary glands from control mice or mice treated with sunitinib. Data are means ± s.d. (n=4-8; **P<0.005; ***P<0.0005; One-Way ANOVA to *NeuT;Apln*$^{+/+}$). Representative H&E images are shown. **C**, Tumor volume of NeuT+ mammary tumors size-matched at 20-70mm^3 and followed over-time by MRI analysis (n=5-7). Lines are nonlinear fit of tumor growth. **D**, Mitotic count of 6 weeks age-matched tumors from *NeuT;Apln*$^{+/+}$ and *NeuT;Apln*$^{-/-}$ mice, control or treated with sunitinib. Some control mice had to be sacrificed after 4 weeks owing to the tumour size following ethical

guidelines (triangular shapes). Data are means ± s.d. (n=4-9; *P<0.05; One-Way ANOVA to *NeuT;Apln*$^{-/-}$ sunitinib). Representative H&E images are shown.

Although anti-angiogenic treatment initially reduces tumour growth, in the long term, it increases other malignant tumor features [65,66]. We visualized the dynamics of current RTKI anti-angiogenic therapy and apelin targeting on tumor vascularity over time using MRI. First, size-matched early stage tumors were imaged by MRI after 2, 4 and 6 weeks and the relative tumour blood volume (rTBV) was assessed. Whereas control *NeuT;Apln*$^{+/+}$ tumors show an increase in blood volume over time, sunitinib treatment reduces vascularity especially at the mid-term point (4 wks) (Figure 10A). This analysis was confirmed by CD31 immunostaining of microvessel density in 4 wk age-matched tumors (Figure 10B). *NeuT;Apln*$^{-/-}$ tumors also exhibited reduced blood volumes following similar kinetics to sunitinib-treated *NeuT;Apln*$^{+/+}$ tumors, although this was only significant in CD31 vessel density. Sunitinib-treated *NeuT;Apln*$^{-/-}$ tumors showed a trend towards reduced vessel density and blood volume compared to control *NeuT;Apln*$^{+/+}$ tumors but, unlike sunitinib therapy alone, it was consistently maintained over time (Figure 10A,B). This data shows that both absence of apelin and blockage of the VEGF pathway by RTKI can reduce tumor angiogenesis and that a combination of both have extended effects.

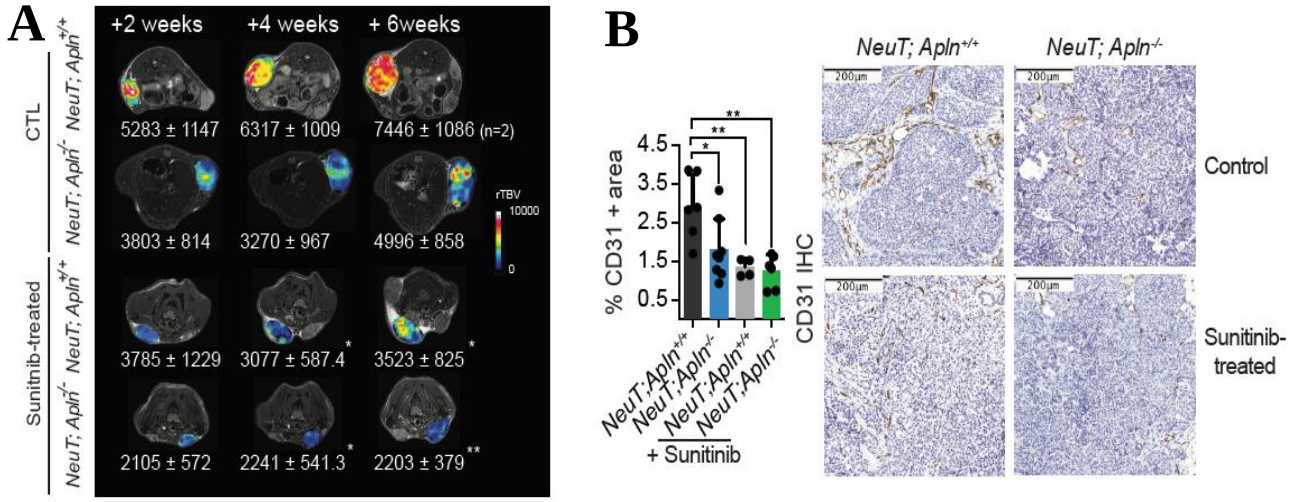

Figure 10. VEGFR and Apelin cooperate in establishing the tumor vasculature. A, MRI analysis of relative tumor blood volume (rTBV) over-time after NeuT+ mammary tumors were size-matched at 20-70mm^3. Data are shown as means ± s.e.m from 4 different tumors. In *NeuT;Apln*$^{+/+}$ only 2 tumors were measured after 6 weeks as some mice had to be previously sacrificed owing to the tumor size following ethical guidelines.

Significance to *NeuT;Apln*$^{+/+}$ is shown (*P<0.05; **P<0.005; one-way ANOVA). **B,** Percentage of CD31+ area in *NeuT;Apln*$^{+/+}$ and *NeuT;Apln*$^{-/-}$ 4 weeks age-matched mammary tumors, control or treated with sunitinib. Representative CD31 stainings are shown. Data are means ± s.d. (n=4-8; *P<0.05; **P<0.005; one-way ANOVA).

The ability of anti-angiogenesis treatment to reduce tumor vascular supply has proven to have a limited anti-tumour efficacy. To overcome the resistance to VEGF-targeted therapies, which produce initial responses in tumor growth that are followed by increased tumour progression and metastasis [41], strategies to potentiate vessel normalization are a promising concept. As we found that tumor apelin blockage could reduce not only microvessel density but also vessel leakage, which was supported by our transcriptome and pathway analysis results in mouse and human endothelial cells, we next aimed to functionally study the dynamics of vessel permeability over time upon RTKI anti-angiogenic treatment and apelin targeting by MRI. Again, size-matched *Apln*$^{+/+}$ and *Apln*$^{-/-}$ NeuT+ mammary tumours at the onset of disease were treated or untreated with sunitinib and followed over time (2, 4 and 6 weeks). Systematic DSC post-contrast perfusion analysis in viable tumour tissue by MRI revealed that control *NeuT;Apln*$^{+/+}$ tumours are visibly leaky from their early development onwards, with the larger tumours being leakier (K_2) (Figure 11A), showing that tumor vessel permeability is linked with tumor progression. Sunitinib-treated *NeuT;Apln*$^{+/+}$ tumours showed a rather high but constant vessel leakage; apelin ablation counteracted sunitinib-induced tumour vessel leakiness (Figure 11A). We also quantified T_2 measurements in viable NeuT+ mammary tumour tissue. Increased T_2 values are attributable to hypoxia (low pO_2), changes in pH (acidosis), increased water content and/or decreased macromolecular content, and therefore elevated T_2 values are linked with increased tumour malignancy. We found that apelin deficiency significantly decreases T_2 values and, most significantly, counteracts any sunitinib-induced T_2 increase (Figure 11A). 3D reconstruction of contrast agent accumulation in representative mammary tumours over time allowed the 3D visualization of necrotic regions with blood pools, where the areas with the highest signal intensity represent the greatest accumulation of contrast agent (Figure 11B). Signal intensities in the areas outside necrotic regions correlate with microvascular leakiness and K_2 values. As visualized in fast-growing control *NeuT;Apln*$^{+/+}$ tumors, contrast agent accumulation, and therefore necrosis and vessel permeability, increases with tumor progression.

Sunitinib treatment in *NeuT;Apln*$^{+/+}$ mice also showed a general contrast accumulation, which increased with tumor size as in control *NeuT;Apln*$^{-/-}$ tumors. Only sunitinib-treated *NeuT;Apln*$^{-/-}$ tumours showed no contrast accumulation even after 6 weeks, which was consistent with fewer necrotic areas in the combinatory scenario (Figure 11A,B). These results also correlated with the histological grade of the tumour and the absence of dilated intratumoral vessels (Figure 11C). These results show that apelin blockage can potentiate sunitinib's inhibition of tumor growth and that apelin loss can reduce the undesirable effects of RTKI therapy, such as increased vessel permeability, hypoxia, necrosis and malignancy, in the primary tumour.

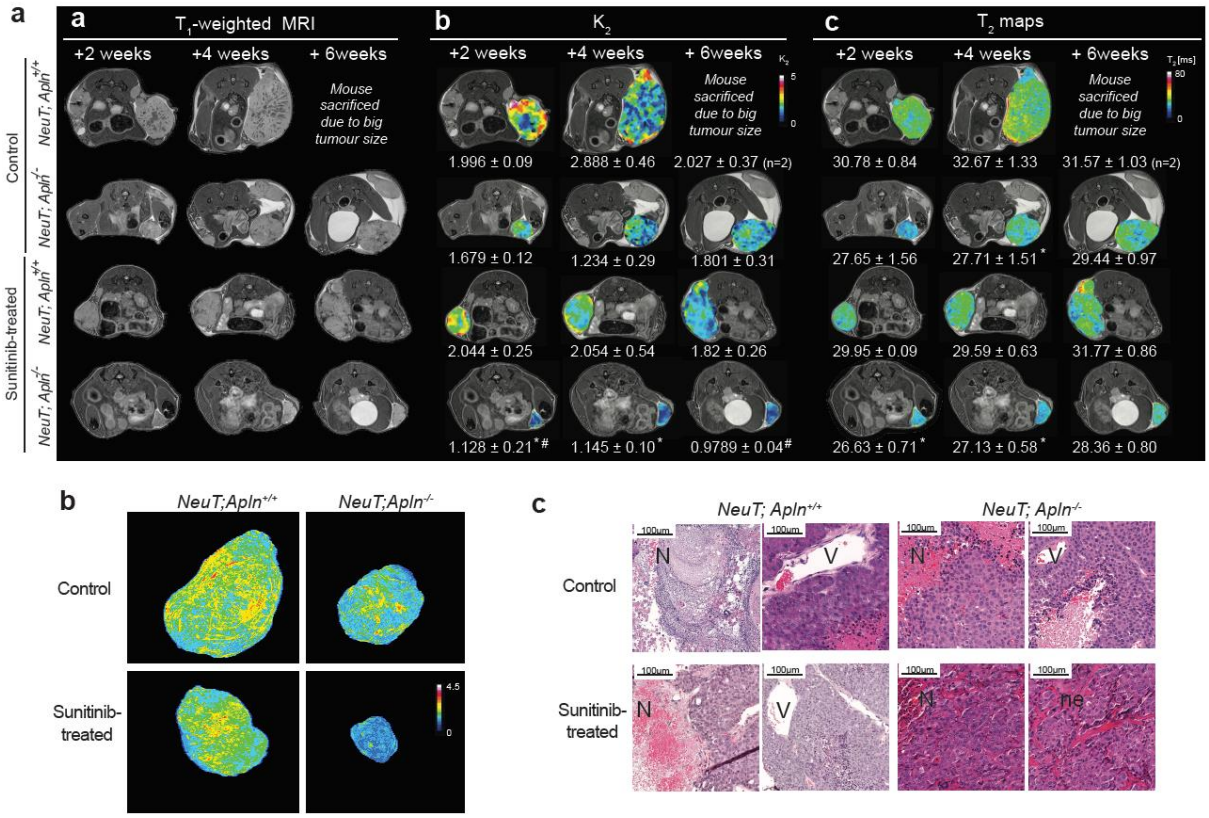

Figure 11. Combination of apelin and RTK blockage reduces vessel leakage and malignancy. A, MRI scans of the center slice (subpanel a) and analysis of K_2 leakage pre/post contrast normalized to muscle (subpanel b) and T_2 maps (subpanel c) in viable tumour tissue of NeuT+ mammary tumors size-matched at 20-70mm^3 and followed-over time after 2, 4 and 6 weeks. Necrotic areas seen as black areas in MRI scans were avoided as they lack tumour vasculature. Data are means ± s.e.m from 4 different tumors and representative images are presented. In *NeuT;Apln*$^{+/+}$ only 2 tumors were measured after 6 weeks as some mice had to be previously sacrificed owing to the tumor size following ethical guidelines ($P<0.05$ significance to *NeuT;Apln*$^{+/+}$ (*) or sunitinib-treated *NeuT;Apln*$^{+/+}$ ($^{\#}$); one-way ANOVA). **B**, Representative T1-weighted post contrast images after 6 weeks, or 4 weeks in the case of *NeuT;Apln*$^{+/+}$ control, 3 min post i.v. magnevist injection rendered in 3D and pseudo colored. The color scale represents signal intensity normalized to muscle. Areas with the highest signal intensity represent contrast agent accumulation within blood pools in the necrotic regions of the tumor. Signal intensities in the areas outside necrotic regions correlate with microvascular leakiness and K_2 values. **C,** Histological features of NeuT+ tumours followed

by MRI. All tumours are age-matched at 6 weeks but for control *NeuT;Apln*$^{+/+}$, as the mouse had to be sacrificed after 4 weeks owing to the tumour size following ethical guidelines.. N= necrosis with associated haemorrhage. V= dilated intratumoural vessels. ne= such vessels are typically not evident.

In addition to the impact of anti-angiogenesis therapy on the primary tumour, metastases have been shown to increase with the use of VEGF pathway inhibitors, including sunitinib therapy, although a reduction in primary tumour growth occurs at the same time [65,66]. We therefore evaluated the number of lung metastatic foci in mice with NeuT+ tumours. To match this result with the vascular MRI data, we analysed the lungs from tumour-bearing mice after 6 weeks after the tumours were size-matched. As in previous studies, we observed that sustained sunitinib treatment significantly increases the number of metastases [65,66], but apelin targeting dramatically reduced their number (Figure 12), thereby overcoming one of the key features of resistance to anti-VEGF or multimodal RTKI anti-angiogenic treatment.

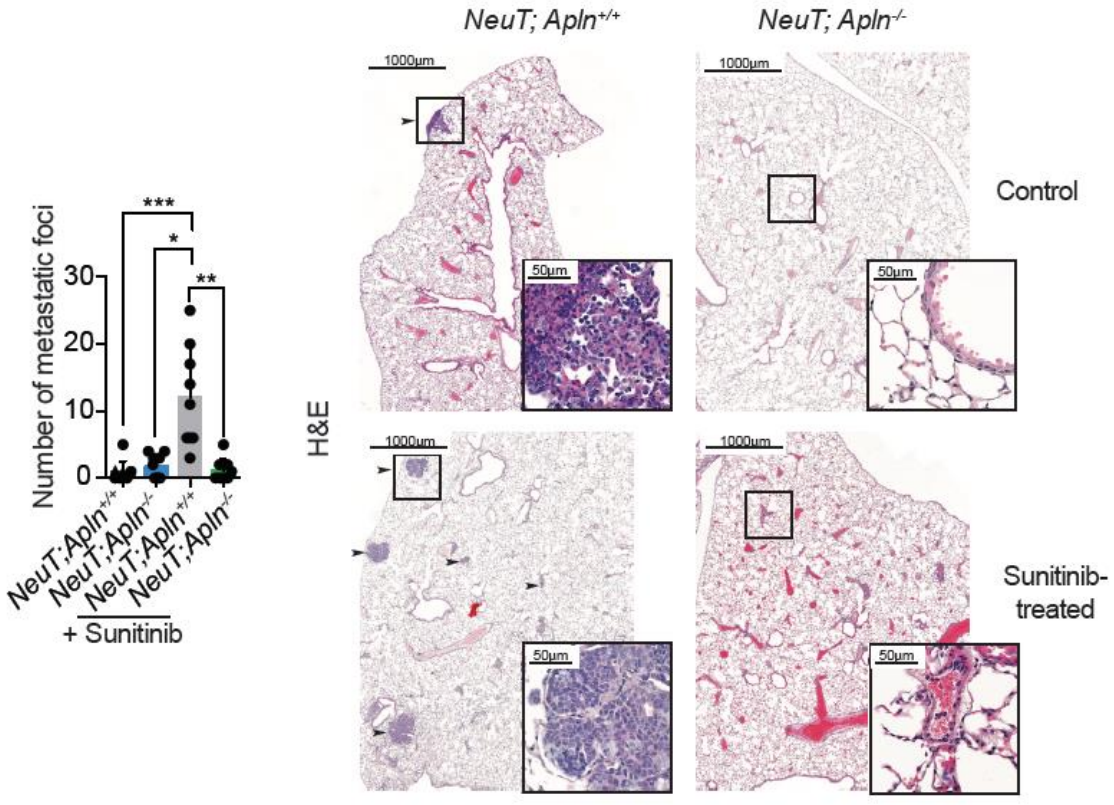

Figure 12. Apelin targeting subdues anti-angiogenic RTKI-induced metastasis. Number of metastatic lung foci from NeuT+ mammary tumors 6 weeks age-matched after tumour onset. Data are shown as means ± s.d (*P<0.05; **P<0.005; ***P<0.0005; Kruskal-Wallis test; n=3, three longitudinal levels per lung). Right panels show representative images of lung metastases in the indicated mice and treatments.

We confirmed and extended this result using the E0771 orthotopic mammary cancer model, which showed similar results in tumour growth upon sunitinib treatment (Figure 13A). Histological analysis of metastatic foci in the lungs of mice sacrificed with large size-matched tumours showed that tumour apelin blockage significantly reduced anti-angiogenic sunitinib-treatment-induced metastasis (Figure 13B,C). Taken together, these results confirm that targeting apelin reduces the metastatic potential of tumors treated with RTKI anti-angiogenic therapy.

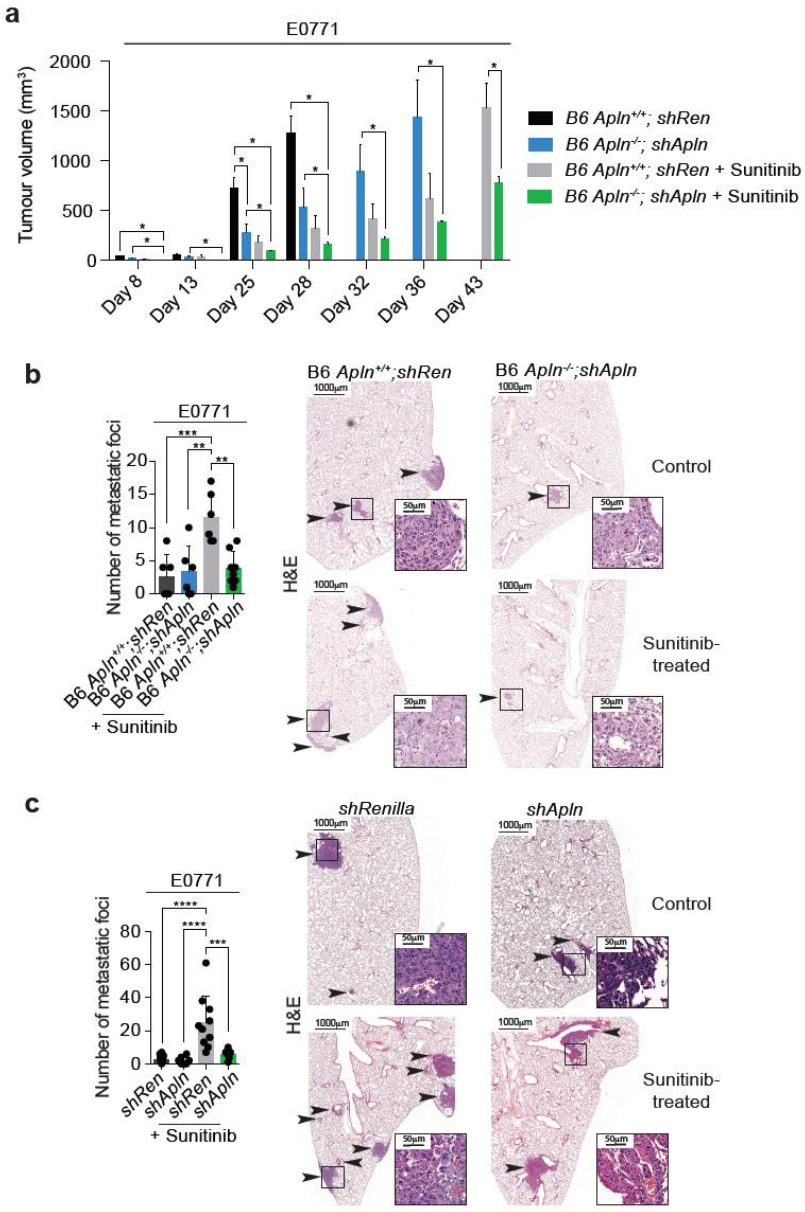

Figure 13. Targeting apelin reduces metastases of breast tumors treated with anti-VEGF therapy. A, Volume of mammary tumors from E0771 control (*shRen*) and apelin-interfered (*shApln.2038*) cells orthotopically-injected in C57B6/J *Apln*$^{+/+}$ or *Apln*$^{-/-}$ mice, as indicated. Data are shown as means ± s.e.m. (n=3-4; *P<0.05, multiple t tests). **B**, Number of metastatic lung foci from 1.5cm^3 size-matched E0771 control (*shRen*) and apelin-interfered (*shApln.2038*) tumours orthotopically-injected in C57B6/J *Apln*$^{+/+}$ or *Apln*$^{-/-}$ mice, as indicated. Data are shown as means ± s.d (**P<0.005; ***P<0.0005; One-way ANOVA; n=3, two longitudinal levels per lung). **C**, Number of metastatic lung foci from 1.5cm^3 size-matched E0771 control (*shRen*) and apelin-interfered (*shApln.2038*) tumours orthotopically-injected in C57B6/J mice. Data are shown as means ± s.d (**P<0.005; ***P<0.0005; One-way ANOVA; n=3, two longitudinal levels per lung).

Discussion. Cancer switches on angiogenesis. Initial attempts to switch off tumor angiogenesis therapeutically were thwarted by resistance and side effects. Our findings unveil a new strategy combining RTK inhibition (i.e. of the VEGFR pathway) with GPCR inhibition (i.e. of the apelin signalling pathway) to diminish tumor growth, microvessel density, vessel abnormality and thus tumor malignancy and therapy-induced metastasis. We have shown here that both pathways, namely VEGF and Apelin, control angiogenesis and vessel permeability. As the apelin signalling pathway is mostly relevant during developmental angiogenesis and is specifically upregulated in tumors, the toxic effects of the pathway blockage are predicted to be minimal. Toxicity is a relevant issue often associated with anti-cancer treatments including anti-angiogenic therapy. Evidence for a lack of toxicity is the fact that *Apln*$^{-/-}$ mice are viable and healthy in adulthood, which shows that apelin signalling blockage is compatible with life. Our transcriptome results in sprouting endothelial cells suggest that apelin is also necessary to regulate TNF and TGFβ1-target genes. This finding could also explain why apelin and VEGF targeting present different kinetics of microvessel density and leakage. In addition, and more strikingly, blockage of apelin in combination with RTKI potentiates its anti-angiogenic effects and significantly reduces the malignant features associated with therapy resistance. Apelin targeting in addition to VEGF RTKI would not only reduce the growth and malignant progression of the primary tumor through maintenance of a less abnormal tumor vasculature, but would also decrease the impact on metastasis, which is usually the main cause of death in breast cancer.

KEY RESEARCH ACCOMPLISHMENTS:

- **Serum analysis of RANKL, OPG and Progesterone in different breast cancer cohorts**
- **In postmenopausal women without known genetic predisposition, high RANKL and progesterone serum levels stratify a subpopulation of women at high risk of developing breast cancer 12-24 months before diagnosis (5.33-fold risk, 95%CI 1.5-25.4; *P*=0.02).**
- **In women with established breast cancer, we demonstrate that RANKL/OPG ratios change dependent on the presence of circulating tumor cells (CTCs).**
- **In a prospective human breast cancer cohort, alterations in RANKL/OPG ratios are significantly associated with breast cancer manifestation.**
- **These data indicate that the RANKL/RANK/OPG system is deregulated in post-menopausal women at high risk for breast cancer and in women with circulating tumor cells.**
- **Serum levels of RANKL/OPG are potentially indicative of predisposition and progression of breast cancer in humans.**
- **Identification of Apelin as a key regulator of tumor neo-angiogenesis in breast cancer**
- **Demonstration that Apelin is invovled in VEGFR-mediated blood vessel growth**
- **Targeting Apelin reduces the metastatic potential of tumors treated with current RTKI anti-angiogenic therapy**
- **Apelin is a potential novel target for cancer treatment**

REPORTABLE OUTCOMES:

Our paper reporting the role of RANKL/RANK in BRCA1-driven breast cancer has now been published (Sigl et al. Cell Reports) and the data outlined in this report are accepted (pending final revisions) in Oncotarget. The work on Apelin in angiogenesis is being prepared for submission.

CONCLUSIONS. Neo-angiogenesis, the sprouting of new blood vessels from the existing vasculature, is one of the hallmarks of cancer and facilitates rapid tumour growth and metastasis. Thus, inhibiting tumour neo-angiogenesis is a strategy for cancer treatment currently being pursued. However, development of resistance and tumor pro-angiogenic responses to current anti-VEGF-targeted therapies limits its efficiency in cancer treatment. Thus, efforts are being invested to find new pro-angiogenic factors to be targeted in cancer, either alone or in combinatorial therapies. Apelin is an evolutionary conserved peptide that acts as the endogenous ligand for the G-protein-coupled APJ receptor. The apelin/APJ signalling pathway has been previously shown to play a role in vascular development and apelin has been found frequently upregulated in mouse and human tumors. Combining tissue engineering and our repairable haploid stem cells, we have now managed to develop 3D blood vessel organoids which allowed us to identify Apelin as an essential gene required for VEGFR induced blood vessel sprouting. Our experiments indicate that genetic ablation of Apelin indeed affects tumor neo-angiogenesis and improves survival in our NeuT-induced mammary cancer model. Moreover, Apelin appears to cooperate with VEGFR in blood vessel quality control and blood vessel leakiness in mammary cancers. Thus, we have identified apelin as a potential novel target for breast cancer treatment.

Secondly, we have previously identified RANKL/RANK as a key “missing link” between sex hormones and the initiation of mammary cancer and recently expanded this finding to cancer driven by BRCA1 mutations. Our results in mouse models indicate that genetic ablation of RANK markedly delays and in some cases even abolishes the development of BRCA1/p53 mutation-driven mammary cancer. Since an anti-RANKL blocking antibody has already been approved for human use, our data provide a rationale for clinical trials to possibly prevent the development of triple negative breast cancer –a phase III clinical trial is currently being initiated, translating our basic findings to hopefully true prevention of breast cancer. Our human serology data, presented in this report in detail, indicate that the RANKL/RANK/OPG system is deregulated in post-menopausal women at high risk for breast cancer and in women with

circulating tumor cells. Thus, serum levels of RANKL/OPG are potentially indicative of predisposition and progression of breast cancer in humans.

REFERENCES

1. Kong YY, Yoshida H, Sarosi I, et al. OPGL is a key regulator of osteoclastogenesis, lymphocyte development and lymph-node organogenesis. Nature. 1999; 397(6717): 315-323.
2. Wada T, Nakashima T, Hiroshi N, Penninger JM. RANKL-RANK signaling in osteoclastogenesis and bone disease. Trends in Molecular Medicine. 2006; 12(1): 17-25.
3. Cummings SR, San Martin J, McClung MR, et al. Denosumab for prevention of fractures in postmenopausal women with osteoporosis. The New England Journal of Medicine. 2009;3 61(8): 756-765.
4. Fizazi K, Carducci M, Smith M, et al. Denosumab versus zoledronic acid for treatment of bone metastases in men with castration-resistant prostate cancer: a randomised, double-blind study. Lancet. 2011; 377(9768): 813-822.
5. Henry DH, Costa L, Goldwasser F, et al. Randomized, double-blind study of denosumab versus zoledronic acid in the treatment of bone metastases in patients with advanced cancer (excluding breast and prostate cancer) or multiple myeloma. Journal of Clinical Oncology. 2011; 29(9): 1125-1132.
6. McClung MR, Lewiecki EM, Cohen SB, et al. Denosumab in postmenopausal women with low bone mineral density. The New England Journal of Medicine. 2006; 354(8): 821-831.
7. Smith MR, Egerdie B, Hernandez Toriz N, et al. Denosumab in men receiving androgen-deprivation therapy for prostate cancer. The New England Journal of Medicine. 2009; 361(8): 745-755.
8. Dougall WC, Glaccum M, Charrier K, et al. RANK is essential for osteoclast and lymph node development. Genes & Development. 1999; 13(18): 2412-2424.
9. Rossi SW, Kim MY, Leibbrandt A, et al. RANK signals from CD4(+)3(-) inducer cells regulate development of Aire-expressing epithelial cells in the thymic medulla. The Journal of Experimental Medicine. 2007; 204(6): 1267-1272.
10. Fata JE, Kong YY, Li J, et al. The osteoclast differentiation factor osteoprotegerin-ligand is essential for mammary gland development. Cell. 2000; 103(1): 41-50.
11. Fernandez-Valdivia R, Mukherjee A, Ying Y, et al. The RANKL signaling axis is sufficient to elicit ductal side-branching and alveologenesis in the mammary gland of the virgin mouse. Developmental Biology. 2009; 328(1): 127-139.

12. Schramek D, Leibbrandt A, Sigl V, et al. Osteoclast differentiation factor RANKL controls development of progestin-driven mammary cancer. Nature. 2010; 468(7320): 98-102.
13. Gonzalez-Suarez E, Jacob AP, Jones J, et al. RANK ligand mediates progestin-induced mammary epithelial proliferation and carcinogenesis. Nature. 2010; 468(7320): 103-107.
14. Sigl V. et al. RANKL/RANK control Brca1 mutation-driven mammary tumors. Cell Research 2016; 26: 761-774.
15. Nolan E, et al. RANK ligand as a potential target for breast cancer prevention in BRCA1-mutation carriers. Nature Medicine. 2016 22(8):933-939.
16. Tanos T, Sflomos G, Echeverria PC, Ayyanan A, Gutierrez M, Delaloye JF, Raffoul W, Fiche M, Dougall W, Schneider P, Yalcin-Ozuysal O, Brisken C. Progesterone/RANKL is a major regulatory axis in the human breast. Science Translational Medicine. 2013; 5(182): 182ra55.
17. Asselin-Labat ML, Vaillant F, Sheridan JM, et al. Control of mammary stem cell function by steroid hormone signalling. Nature. 2010; 465(7299): 798-802.
18. Joshi PA, Jackson HW, Beristain AG, et al. Progesterone induces adult mammary stem cell expansion. Nature. 2010; 465(7299): 803-807.
19. Jones DH, Nakashima T, Sanchez OH, et al. Regulation of cancer cell migration and bone metastasis by RANKL. Nature. 2006; 440(7084): 692-696.
20. Tan W, Zhang W, Strasner A, et al. Tumour-infiltrating regulatory T cells stimulate mammary cancer metastasis through RANKL-RANK signalling. Nature. 2011; 470(7335): 548-553.
21. Ferlay J, Autier P, Boniol M, Heanue M, Colombet M, Boyle P. Estimates of the cancer incidence and mortality in Europe in 2006. Annals of oncology : official journal of the European Society for Medical Oncology / ESMO. 2007; 18(3): 581-592.
22. Jemal A, Siegel R, Ward E, Hao Y, Xu J, Thun MJ. Cancer Statistics. 2009; 59(4): 225-249.
23. Van Poznak C, Cross SS, Saggese M, et al. Expression of osteoprotegerin (OPG), TNF related apoptosis inducing ligand (TRAIL), and receptor activator of nuclear factor kappaB ligand (RANKL) in human breast tumours. Journal of Clinical Pathology. 2006; 59(1): 56-63.
24. Menon U, Gentry-Maharaj A, Hallett R, et al. Sensitivity and specificity of multimodal and ultrasound screening for ovarian cancer, and stage distribution of detected cancers: results of the prevalence screen of the UK Collaborative Trial of Ovarian Cancer Screening (UKCTOCS). The Lancet Oncology. 2009; 10(4): 327-340.
25. Menon U, Gentry-Maharaj A, Ryan A, et al. Recruitment to multicentre trials--lessons from UKCTOCS: descriptive study. BMJ. 2008; 337: a2079.

26. Cristofanilli M, Hayes DF, Budd GT, et al. Circulating tumor cells: a novel prognostic factor for newly diagnosed metastatic breast cancer. Journal of Clinical Oncolology. 2005; 23(7): 1420-1430.
27. Cristofanilli M, Budd GT, Ellis MJ, et al. Circulating tumor cells, disease progression, and survival in metastatic breast cancer. The New England Journal of Medicine. 2004; 351(8): 781-791.
28. Kiechl S, Schett G, Schwaiger J, et al. Soluble receptor activator of nuclear factor-kappa B ligand and risk for cardiovascular disease. Circulation. 2007; 116(4): 385-391.
29. Kiechl S, Schett G, Wenning G, et al. Osteoprotegerin is a risk factor for progressive atherosclerosis and cardiovascular disease. Circulation. 2004; 109(18): 2175-2180.
30. Key T, Appleby P, Barnes I, Reeves G. Endogenous sex hormones and breast cancer in postmenopausal women: reanalysis of nine prospective studies. Journal National Cancer Institute 2002; 94(8)606-616.
31. Schett G, Kiechl S, Redlich K et al. Soluble RANKL and risk of nontraumatic fracture. *JAMA* 2004; 291:1108-1113.
32. Jorgensen L, Vik A, Emaus N et al. Bone loss in relation to serum levels of osteoprotegerin and nuclear factor-kappaB ligand: the Tromso Study. Osteoporosis International 2010; 21:931-938.
33. Mountzios G, Dimopoulos MA, Bamias A, et al. Abnormal bone remodeling process is due to an imbalance in the receptor activator of nuclear factor-kappaB ligand (RANKL)/osteoprotegerin (OPG) axis in patients with solid tumors metastatic to the skeleton. Acta Oncologia 2007; 46: 221-229.
34. Huesemann et al, Systemic spread is an early step in breast cancer. Cancer Cell. 2008;13(1): 58-68.
35. Akhtari M, Mansuri J, Newman KA, Guise TM, Seth P. Biology of breast cancer bone metastasis.Cancer Biology Therapy. 2008; 7(1): 3-9.
36. Gnant M, Pfeiler G, Dubsky PC, Hubalek M, Greil R, Jakesz R, Wette V, Balic M, Haslbauer F, Melbinger E, Bjelic-Radisic V, Artner-Matuschek S, Fitzal F, Marth C, Sevelda P, Mlineritsch B, Steger GG, Manfreda D, Exner R, Egle D, Bergh J, Kainberger F, Talbot S, Warner D, Fesl C, Singer CF; Austrian Breast and Colorectal Cancer Study Group. Adjuvant denosumab in breast cancer (ABCSG-18): a multicentre, randomised, double-blind, placebo-controlled trial. Lancet. 2015; 386(9992): 433-443.
37. Widschwendter M, Burnell M, Fraser L, Rosenthal AN, Philpott S, Reisel D, Dubeau L, Cline M, Pan Y, Yi PC, Gareth Evans D, Jacobs IJ, Menon U, Wood CE, Dougall WC. Osteoprotegerin (OPG), The Endogenous Inhibitor of Receptor Activator of NF-κB Ligand (RANKL), is Dysregulated in BRCA Mutation Carriers. EBioMedicine. 2015;

2(10):1331-1339.

38. Hanahan, D. & Weinberg, R. A. Hallmarks of Cancer: The Next Generation. *Cell* 144, 646–674 (2011).
39. Carmeliet, P. & Jain, R. K. Molecular mechanisms and clinical applications of angiogenesis. *Nature* 473, 298–307 (2011).
40. Potente, M., Gerhardt, H. & Carmeliet, P. Basic and Therapeutic Aspects of Angiogenesis. *Cell* 146, 873–887 (2011).
41. Bergers, G. & Hanahan, D. Modes of resistance to anti-angiogenic therapy. *Nat Rev Cancer* 8, 592–603 (2008).
42. Jain, R. K. Normalizing tumor vasculature with anti-angiogenic therapy: a new paradigm for combination therapy. *Nat Med* 7, 987–989 (2001).
43. Carmeliet, P. & Jain, R. K. Principles and mechanisms of vessel normalization for cancer and other angiogenic diseases. *Nature Publishing Group* 10, 417–427 (2011).
44. Rivera, L. B. & Bergers, G. CANCER. Tumor angiogenesis, from foe to friend. *Science* 349, 694–695 (2015).
45. Tatemoto, K. *et al.* Isolation and characterization of a novel endogenous peptide ligand for the human APJ receptor. *Biochemical and Biophysical Research Communications* 251, 471–476 (1998).
46. Kidoya, H. & Takakura, N. Biology of the apelin-APJ axis in vascular formation. *J Biochem* (2012). doi:10.1093/jb/mvs071
47. Saint-Geniez, M., Masri, B., Malecaze, F., Knibiehler, B. & Audigier, Y. Expression of the murine msr/apj receptor and its ligand apelin is upregulated during formation of the retinal vessels. *Mech. Dev.* 110, 183–186 (2002).
48. Cox, C. M., D'Agostino, S. L., Miller, M. K., Heimark, R. L. & Krieg, P. A. Apelin, the ligand for the endothelial G-protein-coupled receptor, APJ, is a potent angiogenic factor required for normal vascular development of the frog embryo. *Developmental Biology* 296, 177–189 (2006).
49. Kälin, R. E. *et al.* Paracrine and autocrine mechanisms of apelin signaling govern embryonic and tumor angiogenesis. *Developmental Biology* 305, 599–614 (2007).
50. Kasai, A. *et al.* Apelin Is a Crucial Factor for Hypoxia-Induced Retinal Angiogenesis. *Arteriosclerosis, Thrombosis, and Vascular Biology* 30, 2182–2187 (2010).
51. Kidoya, H. *et al.* Spatial and temporal role of the apelin/APJ system in the caliber size regulation of blood vessels during angiogenesis. *EMBO J* 27, 522–534 (2008).
52. del Toro, R. *et al.* Identification and functional analysis of endothelial tip cell-enriched genes. *Blood* 116, 4025–4033 (2010).
53. Kasai, A. *et al.* Apelin is a novel angiogenic factor in retinal endothelial cells. *Biochemical and Biophysical Research Communications* 325, 395–400 (2004).
54. Sorli, S. C., Le Gonidec, S., Knibiehler, B. & Audigier, Y. Apelin is a potent activator of

tumour neoangiogenesis. *Oncogene* 26, 7692–7699 (2007).
55. Berta, J. *et al.* Apelin expression in human non-small cell lung cancer: role in angiogenesis and prognosis. *J Thorac Oncol* 5, 1120–1129 (2010).
56. Seaman, S. *et al.* Genes that Distinguish Physiological and Pathological Angiogenesis. *Cancer Cell* 11, 539–554 (2007).
57. Kuba, K. *et al.* Impaired Heart Contractility in Apelin Gene Deficient Mice Associated With Aging and Pressure Overload. *Circulation Research* 101, e32–e42 (2007).
58. Lucchini, F. *et al.* Early and multifocal tumors in breast, salivary, harderian and epididymal tissues developed in MMTY-Neu transgenic mice. *Cancer Lett.* 64, 203–209 (1992).
59. Liu, Q. *et al.* Genetic targeting of sprouting angiogenesis using Apln-CreER. *Nat Commun* 6, 6020 (2015).
60. Wang, Z., Greeley, G. H., Jr & Qiu, S. Immunohistochemical localization of apelin in human normal breast and breast carcinoma. *J Mol Hist* 39, 121–124 (2007).
61. Pauli, A. *et al.* Toddler: an embryonic signal that promotes cell movement via Apelin receptors. *Science* 343, 1248636 (2014).
62. Jakobsson, L. *et al.* Endothelial cells dynamically compete for the tip cell position during angiogenic sprouting. *Nat. Cell Biol.* 12, 943–953 (2010).
63. Elling, U. *et al.* Forward and Reverse Genetics through Derivation of Haploid Mouse Embryonic Stem Cells. *Cell Stem Cell* 9, 563–574 (2011).
64. Sulzmaier, F. J., Jean, C. & Schlaepfer, D. D. FAK in cancer: mechanistic findings and clinical applications. *Nature Publishing Group* 14, 598–610 (2014).
65. Ebos, J. M. L. *et al.* Accelerated metastasis after short-term treatment with a potent inhibitor of tumor angiogenesis. *Cancer Cell* 15, 232–239 (2009).
66. Pàez-Ribes, M. *et al.* Antiangiogenic therapy elicits malignant progression of tumors to increased local invasion and distant metastasis. *Cancer Cell* 15, 220–231 (2009).

APPENDICES:

Statistics. For the Kaplan-Meier analysis of tumor onset a log rank test was performed. $P < 0.05$ was accepted as statistically significant.

SUPPORTING DATA:

All relevant data are shown in the main description of the tasks.

Publications

Wirnsberger, G., Zwolanek, F., Asaoka, T., Kozieradzki, I., Tortola, L., Wimmer, R.A., Kavirayani, A., Fresser, F., Baier, G., Langdon, W.Y., Ikeda, F., Kuchler, K., and J. M. **Penninger**. Inhibition of CBLB protects from lethal Candida albicans sepsis. **Nature Med.** 22, 915-923. doi: 10.1038/nm.4134. Epub 2016 Jul 18. PMID:27428901. 2016.

Pietrocola, F., Pol, J., Vacchelli, E., Rao, S., Enot, D.P., Baracco, E.E., Levesque, S., Castoldi, F., Jacquelot, N., Yamazaki, T., Senovilla, L., Marino, G., Aranda, F., Durand, S., Sica, V., Chery, A., Lachkar, S., Sigl, V., Bloy, N., Buque, A., Falzoni, S., Ryffel, B., Apetoh, L., Di Virgilio, F., Madeo, F., Maiuri, M.C., Zitvogel, L., Levine, B., **Penninger,** J.M., and G. Kroemer. Caloric Restriction Mimetics Enhance Anticancer Immunosurveillance. **Cancer Cell.** 30, 147-160. doi: 10.1016/j.ccell.2016.05.016. PMID:27411589. 2016.

Sigl, V., Owusu-Boaitey, K., Joshi, P.A., Kavirayani, A., Wirnsberger, G., Novatchkova, M., Kozieradzki, I., Schramek, D., Edokobi, N., Hersl, J., Sampson, A., Odai-Afotey, A., Lazaro, C., Gonzalez-Suarez, E., Pujana, M.A., Cimba, Heyn, H., Vidal, E., Cruickshank, J., Berman, H., Sarao, R., Ticevic, M., Uribesalgo, I., Tortola, L., Rao, S., Tan, Y., Pfeiler, G., Lee, E.Y., Bago-Horvath, Z., Kenner, L., Popper, H., Singer, C., Khokha, R., Jones, L.P., and **J. M. Penninger**. RANKL/RANK control Brca1 mutation-driven mammary tumors. **Cell Res.** 26, 761-774. doi: 10.1038/cr.2016.69. Epub 2016 May 31. PMID:27241552. 2016.

Luo, J., Yang, Z., Ma, Y., Yue, Z., Lin, H., Qu, G., Huang, J, Dai,. W., Li, C., Zheng, C., Xu, L., Chen, H., Wang, J., Li, D., Siwko, S., **Penninger**, J.M., Ning, G., Xiao, J., and M. Liu. LGR4 is a receptor for RANKL and negatively regulates osteoclast differentiation and bone resorption. **Nat Med.** 22, 539-546. doi: 10.1038/nm.4076. Epub 2016 Apr 11. PMID:27064449. 2016.

Tortola, L., Nitsch, R., Bertrand, M.J., Kogler, M., Redouane, Y., Kozieradzki, I., Uribesalgo, I., Fennell, L.M., Daugaard, M., Klug, H., Wirnsberger, G., Wimmer, R., Perlot, T., Sarao, R., Rao, S., Hanada, T., Takahashi, N., Kernbauer, E., Demiröz, D., Superti-Furga, G., Decker, T., Pichler, A., Ikeda, F., Kroemer, G., Vandenabeele, P., Sorensen, P.H., and **J. M. Penninger**. The Tumor Suppressor Hace1 Is a Critical Regulator of TNFR1-Mediated Cell Fate. **Cell Rep.** 15, 1481-1492. doi: 10.1016/j.celrep.2016.04.032. Epub 2016 May 5. PMID: 27160902. 2016.

Nagy, V., and **J. M. Penninger**.The RANKL-RANK Story. **Gerontology**. PMID: 25720990. 2015.

Cheloufi, S., Elling, U., Hopfgartner, B., Jung, Y.L., Murn, J., Ninova, M., Hubmann, M., Badeaux, A.I., Euong Ang, C., Tenen, D., Wesche, D.J., Abazova, N., Hogue, M., Tasdemir, N., Brumbaugh, J., Rathert, P., Jude, J., Ferrari, F., Blanco, A., Fellner, M., Wenzel, D., Zinner, M., Vidal, S.E., Bell, O., Stadtfeld, M., Chang, H.Y., Almouzni, G., Lowe, S.W., Rinn, J., Wernig, M., Aravin, A., Shi, Y., Park, P.J., **Penninger, J.M.,** Zuber, J., and K. Hochedlinger. The histone chaperone CAF-1 safeguards somatic cell identity. **Nature** 528, 218-224. doi: 10.1038/nature15749. 2015.